Characterization of lungs

in a transgenic acid sphingomyelinase mouse model

Inaugural-Dissertation
zur
Erlangung des Doktorgrades

Dr. rer. nat.

der Fakultät für Biologie
an der
Universität Duisburg-Essen

Vorgelegt von

Anne Koch
aus Bad Frankenhausen, Deutschland

2019

Die der vorliegenden Arbeit zugrundeliegenden Versuche wurden am Institut für Molekularbiologie der Universität Duisburg-Essen durchgeführt.

1. Gutachter: Prof. Dr. Katrin Becker-Flegler

2. Gutachter: Prof. Dr. Wiebke Hansen

Vorsitzender des Prüfungsausschusses: Prof. Dr. Nicole Dünker

Tag der mündlichen Prüfung: 04.09.2019

DOI: 10.17185/duepublico/70537
URN: urn:nbn:de:hbz:464-20190910-081030-8

Für Opa.

TABLE OF CONTENTS

CONTENT page

ABBREVIATIONS 7

LIST OF FIGURES 10

LIST OF TABLES 11

ABSTRACT 12

ZUSAMMENFASSUNG 13

1 INTRODUCTION 14

1.1 Biological Membranes 14

1.2 Sphingolipids 14

1.2.1 Metabolism 15

1.2.2 Sphingolipids in diseases 17

1.2.3 Acid sphingomyelinase 23

2 AIM OF THE STUDY 29

3 MATERIALS AND METHODS 30

3.1 Materials 30

3.1.1 Chemicals 30

3.1.2 Antibodies & kits 32

3.1.3 Buffers and solutions 33

3.1.4 Consumables 34

3.1.5 Instruments/equipment 35

3.1.6 Software 36

3.2 Methods 37

3.2.1 Animal husbandry 37
3.2.2 Generation of the transgenic mouse model 37
3.2.3 Acid sphingomyelinase/ acid ceramidase activity assays 38
3.2.4 Lipid quantification 39
3.2.5 Preparation of tissue sections 40
3.2.6 Staining procedures 40
3.2.7 Western Blots 41
3.2.8 Enzyme-linked immunosorbent assays 43
3.2.9 Cytokine array 43
3.2.10 Collagen quantification 44
3.2.11 Statistics 45
4 RESULTS 46
4.1 Mouse model for Asm overexpression 46
4.1.1 Generation of the mouse model 46
4.1.2 Genotypes 46
4.1.3 Physical development of the mice 47
4.2 Sphingolipid metabolism of the lung 48
4.2.1 Enzyme activities 48
4.2.2 Lipid composition 49
4.2.3 Ceramide localization within lung tissue 52
4.3 Pulmonary morphology and histology 53
4.4 Cellular infiltration and lung inflammation 55
4.5 Autophagy 57

5 DISCUSSION 59

6 REFERENCES 68

Acknowledgements 83

Curriculum Vitae 84

Declarations 87

ABBREVIATIONS

AC, Ac	acid ceramidase (human, murine)
AMPK	adenosine monophosphate-activated protein kinase
ANOVA	analysis of variance
AP	alkaline phosphatase
APS	ammonium persulfate
ASM, Asm	acid sphingomyelinase (human, murine)
Atg	autophagy-related
BMP	bis(monoacylglycero)phosphate
BSA	bovine serum albumin
C1P	ceramide-1-phosphate
CAD	cationic amphiphilic drug
cAMP	cyclic adenosine monophosphate
CAPP	ceramide-activated protein phosphatases
CD	cluster of differentiation
CF	cystic fibrosis
CFTR, Cftr	cystic fibrosis transmembrane conductance regulator (human, murine)
CMV	cytomegalovirus
CoA	coenzyme A
cPLA2	cytosolic phospholipase A2
CSF	cerebrospinal fluid
DAG	diacylglycerol
DRM	detergent-resistant membranes
e. g.	*exempli gratia;*for example
ECL	enhanced chemoluminescence
ELISA	enzyme-linked immunosorbent assay
ER	endoplasmic reticulum
f wt / ♀ wt	female wildtype
FELASA	Federations of European Laboratory Animal Science Association
FIASMA	functional inhibitor of ASM

G(M)-CSF	granulocyte-(macrophage) colony stimulating factor
Glc	glucose
GPI	glycosylphophatidylinositol
H&E	hematoxylin & eosin
HAT	hypoxanthine, aminopterin, thymidine
HPLC	high performance liquid chromatography
HPRT	hypoxanthine-guanine phosphoribosyltransferase
HRP	horseradish peroxidase
i. e.	*id est;* in other words
Ig	immunoglobulin
IL	interleukin
KC	keratinocyte chemoattractant
LC	microtubule-associated protein light chain
LPS	lipopolysaccharide
m wt/ ♂ wt	male wildtype
mTOR	mammalian target of rapamycin
NAc	N-acetyl
PBS	phosphate-buffered saline
PFA	paraformaldehyde
pI3K	phosphoinositide 3-kinase?
PI3P	phosphatidylinositol 3-phosphate
PKC	protein kinase C
PP2A	protein phosphatase 2A
RT	room temperature
S1P	sphingosine-1-phosphate
SAP	sphingolipid activator protein
SD	standard deviation
SDS	sodium dodecyl sulfate
SMPD, Smpd	sphingomyelin phosphodiesterase (human, murine)
SPT	serine palmitoyl transferase
TACE	TNFα converting enzyme
tAsm	transgenic Asm mouse strain, Asm transgenic mice

TFEB	transcription factor EB
tg/+	heterozygous
tg/0	hemizygous
tg/tg	homozygous
TNFα	tumor necrosis factor alpha
ULK	unc-51-like kinase
UV	ultraviolet
VPS	vacuolar protein sorting
wt	wildtype

LIST OF FIGURES

FIGURE 1 SPHINGOLIPID METABOLISM AND STRUCTURES 16
FIGURE 2 STAGES OF AUTOPHAGY AND THEIR REGULATION 22
FIGURE 3 *HPRT* "QUICK KNOCK-IN™"APPROACH, GENOWAY 38
FIGURE 4 WEIGHT CURVE 47
FIGURE 5 ASM AND AC ACTIVITIES 48
FIGURE 6 LIPID COMPOSITION OF MURINE LUNGS 50
FIGURE 7 BRONCHIAL CERAMIDE ACCUMULATION 52
FIGURE 8 PULMONARY MORPHOLOGY AND COLLAGEN CONTENT 54
FIGURE 9 INFILTRATING NEUTROPHILS IN MURINE LUNGS 55
FIGURE 10 SERUM AND TISSUE CYTOKINES 57
FIGURE 11 AUTOPHAGY-RELATED PROTEINS 58

LIST OF TABLES

TABLE 1 ANTIBODIES USED FOR WESTERN BLOT ANALYSES 42

TABLE 2 GENOTYPES 47

ABSTRACT

The expression and activity of the acid sphingomyelinase (ASM), a central enzyme of sphingolipid metabolism, has been identified as an important factor in a variety of pathological settings, including major depression as well as inflammatory and infectious diseases.

To study the influence of the ASM in various diseases, Asm knockout mice are being widely used and are well characterized. It is of equal interest, however, to study the effects of increased ASM activity as well as the efficacy of drugs targeting such an overly active ASM. The aim of this dissertation is to characterize genetically modified mice, which constitutively overexpress the acid sphingomyelinase. Special emphasis was placed on examining the lung phenotype of these mice.

The lipid composition was determined using mass spectrometric analysis. Confocal microscopy in conjunction with histological and immunofluorescence stainings were employed to investigate the lungs in more detail with respect to morphology, inflammatory status, and cellular infiltration. The activity of the Asm was assessed using an established enzyme assay. Since the Asm has been shown to control autophagy, proteins associated with this pathway were analyzed as well.

It was shown that the transgenic mice display very high Asm activity compared to wildtype mice. There were no uniformly consistent changes in the lipid composition, however. Overall, the unchallenged transgenic mice did not show a phenotype divergent from that of wildtype mice. For the most part, the mice did not display pathologic alterations in their lung tissue. One notable exception to this is the distribution of ceramide, the product of the reaction catalyzed by Asm, within the lungs. Ceramide accumulations in bronchial epithelial cells are much more prominent in transgenic compared to wildtype mice. The implications of this have been touched upon in previous publications, but bear further investigation.

As the acid sphingomyelinase can be activated by a diverse sets of stressors, the model presented here can be of significance in various fields of study. Numerous pathologies have already been linked to the ASM/ceramide system, which can now be studied using this new model system. As the mice do not differ significantly from wildtype mice, they lend themselves as an ideal model to investigate Asm-related effects specific to the stressor applied.

ZUSAMMENFASSUNG

Die Expression der sauren Sphingomyelinase (ASM), eines zentralen Enzyms im Metabolismus von Sphingolipiden, spielt bei einer Reihe von Erkrankungen, wie zum Beispiel Depressionen, sowie Entzündungs- und Infektionskrankheiten, eine wichtige Rolle.

Bisher wurden vor allem Asm Knockout-Mäuse verwendet, um den Einfluss dieses Enzyms auf verschiedene Krankheiten zu untersuchen. Es ist allerdings von ebenso großer Bedeutung auch den Effekt einer erhöhten ASM-Aktivität und die Effizienz von Medikamenten, die eine solche hyperaktive Sphingomyelinase hemmen sollen, zu ergründen. Ziel dieser Arbeit ist es genetisch veränderte Mäuse zu charakterisieren, die die saure Sphingomyelinase überexprimieren. Dabei soll hier der Fokus auf den Auswirkungen auf die Lunge liegen.

Die enzymatische Aktivität der sauren Sphingomyelinase wurde mittels eines etablierten Enzymassays bestimmt. Die Lipidzusammensetzung der untersuchten Organe wurde mit Hilfe massenspektrometrischer Analysen ermittelt. Durch die mikroskopische Betrachtung histologischer und immunfluoreszenter Färbungen von Gewebeschnitten, wurden die Einflüsse der veränderten Genexpression auf Morphologie, den Entzündungsstatus und die Infiltration von Zellen in das Gewebe untersucht. Da die Asm eine Rolle bei der Autophagie-Kontrolle spielt, wurde ebenfalls analysiert wie sich die erhöhte Asm-Aktivität auf die Expression von Proteinen, welche bei der Autophagie eine Rolle spielen, auswirkt.

Es konnte gezeigt werden, dass die transgenen Mäuse zwar eine erhöhte Asm-Aktivität aufweisen, jedoch kaum Veränderungen in der Lipidzusammensetzung der untersuchten Gewebe. Im Großen und Ganzen zeigen die transgenen Mäuse keine auffälligen Veränderungen gegenüber Wildtyp-Mäusen. Das Lungengewebe der transgenen Mäuse zeigt keine Auffälligkeiten, mit Ausnahme der Verteilung von Ceramid, dem Produkt der ASM-katalysierten Reaktion, im Lungengewebe. In den transgenen Mäusen gibt es deutlich mehr Ceramid in der apikalen Membran bronchialer Epithelzellen als in Wildtyp-Mäusen.

Da die saure Sphingomyelinase durch verschiedenste Stressfaktoren aktiviert wird, eignet sich dieses Mausmodell für Untersuchungen an Mäusen, die spezifischen Stressoren ausgesetzt sind. Das ASM/Ceramid System wurde schon mit verschiedensten Pathologien in Verbindung gebracht. Dieses Modell kann zur Ergründung der Rolle von ASM Hyperaktivität in diversen Kontexten heran gezogen werden, da der Grundzustand der transgenen Mäuse mit dem von Wildtyp-Mäusen vergleichbar ist.

1 INTRODUCTION

1.1 Biological Membranes

Biological membranes are subject to a constant flux – vesicles, small membranous compartments that can be shuttled within the cell (and outside of it), pinch off and fuse with membranes of different organelles as well as the plasma membrane, the final frontier that separates the inside of the cell from its surroundings. These processes are mainly regulated by proteins embedded in the membrane or attached to it via lipid anchors. Proteins can also allow for communication of one side of a membrane with the other, by enabling matter (via specific transporters, channels or pores) or information (via receptors) to cross the membrane. Therefore it is not surprising that initially the proteinaceous parts of membranes were the focus of studies concerning cell signaling processes.

In the fluid mosaic model of biological membranes proposed by Singer and Nicolson in 1972 lipids figured only as the “solvent” for proteins, providing the means to separate the inside from the outside, but not as players in overcoming this separation (Singer and Nicolson 1972). Second messengers in the form of small soluble molecules, such as cyclic adenosine monophosphate (cAMP) had been identified as conveyors of intracellular information by the middle of the previous century (Berthet *et al.* 1957; Sutherland 1970). The notion that lipids could also be employed to relay information in this way took hold later. Diacylglycerol (DAG) was the first lipid molecule to be attributed with such a function when it was shown that it could initiate signal transduction cascades by directly interacting with protein kinase C (PKC) (Kaibuchis *et al.* 1981). By now a range of lipids have been attributed with signaling functions (Newton *et al.* 2016).

1.2 Sphingolipids

It was found that by no means were the membranes of cells and subcellular structures a homogenous mixture of lipids, but rather revealed striking differences, not only in the composition of different organelle membranes or the two leaflets of a bilayer but also within the plane of one leaflet of the membrane. Certain lipids seemed to form distinct domains with properties that set them apart from other parts of the membrane. Simons and Ikonen dubbed

these domains “lipid rafts” (Simons and Ikonen 1997). They were also termed detergent-resistant membranes (DRM) owing to the procedure of their isolation. However, whether rafts and DRMs are equivalent or if the isolation creates artefacts that have nothing much in common with the domains present within living cells is subject to debate (Brown 2006).

The major lipid constituents of these rafts are cholesterol and sphingomyelin (Simons and Ikonen 1997). Sphingomyelin is part of a large interconnected network of sphingolipids, named in the 1880s after the sphinx for their enigmatic nature (Thudichum 1884).

1.2.1 Metabolism

Sphingolipid metabolism has a unique entry as well as a unique exit point, catalyzed by serine palmitoyl transferase (SPT) and sphingosine-1-phosphate (S1P) lyase, respectively. In between those two reactions sphingolipid metabolites are processed and interconverted in a multitude of ways, influencing cell behavior and responses along the way. The hub of this metabolic network is ceramide (Figure 1A), being not only the central metabolite but also serving a pivotal role in a variety of cellular responses.

Ceramide can be generated *de novo* in a series of steps from non-sphingolipid precursors or via breakdown of complex sphingolipids and sphingomyelin. A third route leading to the production of ceramide is the salvage pathway. As implied by the name, this pathway involves the reintroduction of metabolites into the sphingolipid network rather than their breakdown into non-sphingolipid molecules.

Ceramide consists of a sphingoid base (2-amino-4-trans-octadecene-1,3-diol) with an amide-linked acyl chain (Figure 1B). It should be noted that the addition of the acyl chain by (dihydro)ceramide synthases adds a whole new level of complexity to sphingolipid metabolism. The six different isoforms of ceramide synthase show widely different substrate specificities when it comes to the chain length of the fatty acyl-CoA (Levy and Futerman 2010). Naturally occurring sphingolipids have acyl chains varying from 14 to 26 carbon atoms in length (Mullen *et al.* 2012). This layered complexity applies to all acylated metabolites derived from ceramide.

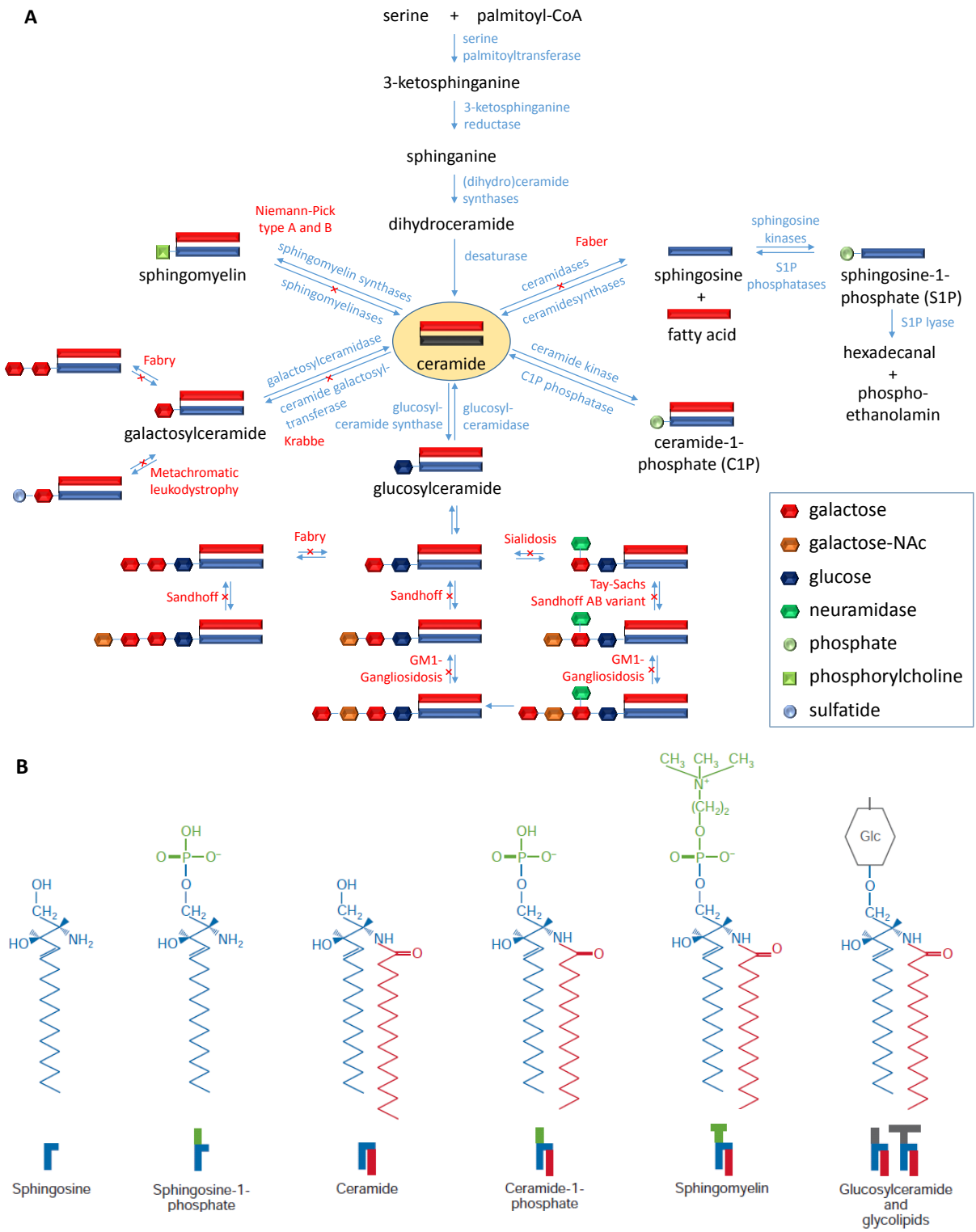

Figure 1 Sphingolipid metabolism and structures
A Overview of sphingolipid metabolism and diseases associated with the deficiencies of certain enzymes. **B** General structures of the major sphingolipids (Futerman and Hannun 2004); Glc - glucose, NAc - N-acetyl

Ceramides can be further processed in a variety of ways – either via modification of their headgroup or deacylation. Modifications of ceramide's headgroup include phosphorylation (ceramide-1-phosphate, C1P), attachment of a phosphorylcholine moiety (sphingomyelin, SM), or glycosylation (complex sphingolipids).

Sphingomyelin is produced mainly in the Golgi apparatus by sphingomyelin synthases. It is a membrane lipid that is particularly enriched in the outer leaflet of the plasma membrane (Testi 1996). As mentioned above it is a major constituent of membrane rafts. Particularly its conversion back to ceramide by sphingomyelinases and the associated changes in membrane fluidity have a huge impact on cellular reactions to external signals (see 1.2.3.2).

Lysosomes are the main location for sphingolipid catabolism to take place. Sphingomyelin and complex sphingolipids residing within the plasma membrane reach the lysosome via the endocytic pathway. Being the "stomachs" of the cell, lysosomes are equipped with a range of hydrolases to degrade various cellular components into their constituent parts, making them available as building blocks for new cellular materials. They can also fulfill other functions, however. In professional phagocytes, for example, they are crucial for degrading phagocytosed materials, e. g. pathogens or cell debris.

A variety of lysosomal enzymes are involved in the sequential breakdown of complex sphingolipids (Figure 1A). Lysosomal sphingomyelin is hydrolyzed to ceramide and phosphorylcholine by the action of acid sphingomyelinase (ASM in humans; Asm in mice). Acid ceramidase (AC in humans; Ac in mice) catalyzes the deacylation of ceramide to sphingosine. Most of the lysosomal lipid hydrolases require the assistance of activator proteins (sphingolipid activator proteins, SAPs). SAPs have surfaces of hydrophobic amino acids that can interact with membrane lipids and "lift" them out of the membrane, enabling the cleavage of the bond in question (Schulze 2009).

1.2.2 Sphingolipids in diseases

The main genetic diseases associated with sphingolipid metabolism are lysosomal storage diseases. A deficiency in any of the lysosomal hydrolases or their respective activator proteins results in an accumulation of the specific enzyme's substrate (Figure 1A). Most of the lysosomal storage diseases show a spectrum of severity, often including infantile-to juvenile- and adult-on set variants of the respective disease. This is due to varying residual activities of the affected enzymes depending on the mutation involved (Kolter and Sandhoff 2006).

Apart from the genetic diseases caused by the disrupted breakdown of sphingolipids, defects in enzymes involved in the *de novo* synthesis also lead to pathological phenotypes often involving neurologic defects (Gable *et al.* 2010; Simpson *et al.* 2004). Underlying this common

pattern is the fact that in cells of the nervous system sphingolipids in general and gangliosides specifically make up a greater portion of the plasma membrane than in other cell types. Also, the myelin sheaths insulating the axons of neurons are largely made up of galactosylceramides (in the central nervous system) and sphingomyelin (in the peripheral nervous system) (Morell and Quarles 1999).

Sphingolipids that act as signaling molecules within and between cells (e. g. ceramide, S1P) can impact a variety of processes throughout the body. Alterations in sphingolipid levels have been associated with a host of acquired diseases. Among others, there have been reports on the sphingolipid-involvement in multiple sclerosis, Alzheimer's disease, atherosclerosis, diabetes, major depressive disorder, pulmonary and liver diseases as well as bacterial infections (Sic *et al.* 2014; Filippov *et al.* 2012; Haass *et al.* 2015; Kornhuber *et al.* 2009; Scarpa *et al.* 2013; Kasumov *et al.* 2015; Seitz *et al.* 2015).

1.2.2.1 Inflammation

Certain sphingolipids are crucially involved in the body's response to tissue damage and/or pathogen invasions. These processes have to be well balanced, as exacerbated or prolonged inflammatory responses have adverse effects on tissue integrity and immune response mechanisms.

Some receptors or modulatory molecules associated with immune and inflammatory responses are located within lipid rafts. For example, pattern recognition receptors or T-cell receptors can be associated with raft regions in the plasma membrane (Varshney *et al.* 2016; Razzaq *et al.* 2004) or complex sphingolipids themselves can act as receptors for certain microorganisms (Nakayama *et al.* 2013; Iwabuchi 2018).

Different sphingolipid species have been reported to influence inflammatory responses via diverse mechanisms. Ceramide, C1P, and S1P act via different pathways to influence the production and/or release of pro-inflammatory chemokines and cytokines as well as prostaglandins (Nixon 2009). Ceramide synthase knock-out studies have shown effects on tumor necrosis factor alpha (TNFα) receptor 1 internalization and signaling (Ali *et al.* 2013). In a cystic fibrosis (CF) mouse model the accumulation of ceramide has been shown to promote cytokine synthesis and release via activation of the inflammasome (Teichgräber *et al.* 2008; Grassmé *et al.* 2014). Involvement of ceramide in inflammasome activation is cell type dependent, however (Scheiblich *et al.* 2017; Camell *et al.* 2015). Ceramide-1-phosphate can

activate cytosolic phospholipase A2 (cPLA2), thereby promoting the release of arachidonic acid, which is a precursor of eicosanoids (Pettus *et al.* 2004). Lipopolysaccharide(LPS)-induced cytokine release, however, can be inhibited by extracellular C1P (Hankins *et al.* 2011). C1P also regulates the processing of TNFα via TACE (TNFα converting enzyme) (Lamour *et al.* 2011).
Reports on the role of S1P with respect to inflammation show, that its role as well is not so clear cut but rather dependent on cell type and cell state as well as which kinase S1P is generated by. Investigations into the role of sphingosine kinase 1, for example, yielded results as diverse as an increase (Grin'kina *et al.* 2012; Di *et al.* 2010), no effect (Michaud *et al.* 2006), or a reduction (Snider *et al.* 2009; Baker *et al.* 2010) of inflammatory responses.
Lymphocyte trafficking from lymphatic tissues into the blood stream is governed by a S1P gradient, which is sensed by lymphocytes via S1P receptor 1 (Cyster and Schwab 2012; Spiegel and Milstien 2011). Neutrophils are among the first leukocytes to be recruited to sites of infection or tissue damage. This is mediated by the production of chemokines, cytokines and adhesion molecules, cued by pro-inflammatory stimuli which are in part controlled by sphingolipid mediators (Grösch *et al.* 2018). Various molecules of the sphingolipid pathway influence neutrophils throughout their life cycle. Neutrophil activation is inhibited by sphingosine, this includes degranulation, phagocytosis, and the oxidative burst. Sphingosine and acid sphingomyelinase promote neutrophil apoptosis, while S1P and the neutral sphingomyelinase promote neutrophil survival (Ohta *et al.* 1994; Lin *et al.* 2011).
Neutrophils also produce cytokines and other inflammatory factors to modulate the further immune and inflammatory responses (Rosales 2018).

1.2.2.2 Cystic fibrosis

Cystic fibrosis (CF) is the most common autosomal-recessive disease among Caucasians, with one in 2500 newborns being affected (Dodge *et al.* 2007). The lungs of CF patients are characterized by hyperinflammatory conditions: a high burden of neutrophils and an increased expression of proinflammatory cytokines. In CF, however, the neutrophils are unable to clear infections. On the contrary, they contribute to an exacerbation of the inflammatory response. Thus, they promote the vicious cycle of (chronic) inflammation and bacterial and viral infections, which entails progressive tissue damage and ultimately loss of function. In severe forms of CF the failing lungs ultimately necessitate a transplant.

The underlying cause for CF is a defect in the cystic fibrosis transmembrane conductance regulator (*CFTR*) gene. This gene encodes an epithelial chloride channel which also facilitates the transport of bicarbonate ions (Borowitz 2015). Depending on the mutation involved, the disease can vary in severity and can affect multiple organs (lung, pancreas, skin, liver, reproductive organs). While the exact molecular mechanism of how the defect in this anion channel leads to a multi-organ disease is not completely understood, some manifestations can be explained with the altered ion flux and concomitant modifications of pH as well as osmotic water flow (Sathe and Houwen 2017; Singh and Schwarzenberg 2017).

The treatment of CF involves multi-disciplinary teams. For the most part, cystic fibrosis treatments still rely on the early, purely symptomatic interventions: nutritional repletion, airway clearance, treatment of airway infections with antibiotics. With the discovery of inflammation as an independent contributor to CF lung disease (Matthews *et al.* 1980) anti-inflammatory treatment was explored as a fourth pillar of care. Overall, the rigorous regimen of care led to an increase in the mean life-expectancy of CF patients from about 6 months for those born in the 1930s (Davis 2006) to about 50 years for those born today (Deutsches Mukoviszidose-Register 2017). However, lung disease remains the major cause of morbidity and mortality for patients with CF.

Over the last ten to fifteen years the notion that sphingolipids play an important role in the context of CF pulmonary exacerbation has gained traction. First off, ceramide was shown to accumulate in CF lungs and lead to pulmonary inflammation via inflammasome activation and subsequent release of IL-1β and the mouse homologue of IL-8 (Teichgräber *et al.* 2008). Ceramide also contributes to the morphological changes associated with pulmonary fibrosis (Ziobro *et al.* 2013). Concomitantly with the accumulation of ceramides, sphingosine levels were found to be decreased in CF airways, impairing the body's ability to efficiently clear pulmonary infections (Pewzner-Jung *et al.* 2014). This imbalance in sphingolipid metabolites is caused mainly by the downregulation of acid ceramidase, the enzyme that hydrolyses ceramide to sphingosine (Grassmé *et al.* 2017). Recently, it was discovered that S1P plays a role in CF lung pathology as well. It acts as a regulator of the CFTR channel (Malik *et al.* 2015). The inhibition of S1P degradation reduces pulmonary inflammation upon *Pseudomonas aeruginosa* infections in Cftr-deficient mice (Veltman *et al.* 2016).

1.2.2.3 Autophagy

Autophagy is part of normal cellular homeostasis – recycling nutrient subunits (e.g. amino acids) of superfluous or damaged and dysfunctional materials (Nakatogawa *et al.* 2009). However, autophagy can also become necessary to ensure a cell's survival in times of low energy states, as during fasting or prolonged exercise and increased energy needs (Palikaras *et al.* 2018). During infections with certain bacteria autophagosomes can also engulf intracellular pathogens and lead to their destruction (Gomes and Dikic 2014). Recently, autophagy has also been attributed with roles in inflammation (Levine *et al.* 2011; Netea-Maier *et al.* 2016). Dysregulation of autophagy has been implicated in various diseases, including neurodegenerative diseases as well as cancer (Levine and Kroemer 2008).

The autophagic process is initiated by a protein complex that consists of unc-51-like kinase 1 (ULK1) and other autophagy-related proteins (Atgs). ULK1 acts as a kinase on Beclin 1, thereby activating vacuolar protein sorting 34 (VPS34) complex, which is anchored to the pre-autophagosomal membrane. VPS34 acts as a class III phosphatidylinositol 3-kinase, producing phosphatidylinositol 3-phosphate (PI3P) at the site of the nascent autophagosome. Thereupon, proteins can be sorted to the budding autophagosomal membrane (phagophore). In the course of the expansion of the phagophore, microtubule-associated proteins light chain 3 (LC3A, B and C) are lipidated with phosphatidylethanolamine to anchor them in the phagophore membrane. These proteins are not only important for autophagosome closure and fusion with lysosomes, but also for cargo recognition. This is achieved via adaptor proteins like p62. ULK1 activates p62 via phosphorylation. Active p62 recognizes ubiquitinylated proteins and targets them to the growing phagophore via its LC3 interacting regions (LIR) (Lin *et al.* 2013). Once the autophagosomal membrane has been elongated far enough to allow for closure, the maturation process begins, culminating in the fusion of the outer autophagosomal membrane with the lysosomal membrane. Within this newly formed autolysosome the inner membrane of the autophagosome and the contents of the autophagosome are being degraded by various lysosomal hydrolases.

Autophagy is regulated on multiple levels. First off, the formation of the initiating complex and the consequent activation of ULK1 is highly regulated and integrates the signals of multiple upstream pathways (Zachari and Ganley 2017). For example, AMPK (adenosine monophosphate-activated protein kinase) acts as an energy sensor, activating ULK1 when the cell is in an unfavorable energy state (Garcia and Shaw 2017). Another master regulator of autophagy is mTOR (mammalian target of rapamycin). It gets activated by an amino acid-sensing complex on the cytosolic side of lysosomes (Settembre *et al.* 2013). The presence of amino acids leads to activation of mTOR, which in turn prevents autophagy initiation via inhibitory phosphorylations of ULK1 (Kim *et al.* 2011). mTOR also phosphorylates and thereby inactivates TFEB, which regulates the transcription of several proteins involved in autophagy (e.g. ULK1, Beclin 1, LC3, p62) (Settembre and Ballabio 2011). mTOR can be shut off in a variety of ways, for example by AMPK, when the cell is in need of energy or cellular building blocks. Under starvation conditions protein phosphatase 2A (PP2A) has a reduced affinity for Beclin 1, while being more active on ULK1, removing inhibitory phosphorylations, thereby promoting autophagy (Fujiwara *et al.* 2016; Wong *et al.* 2015).

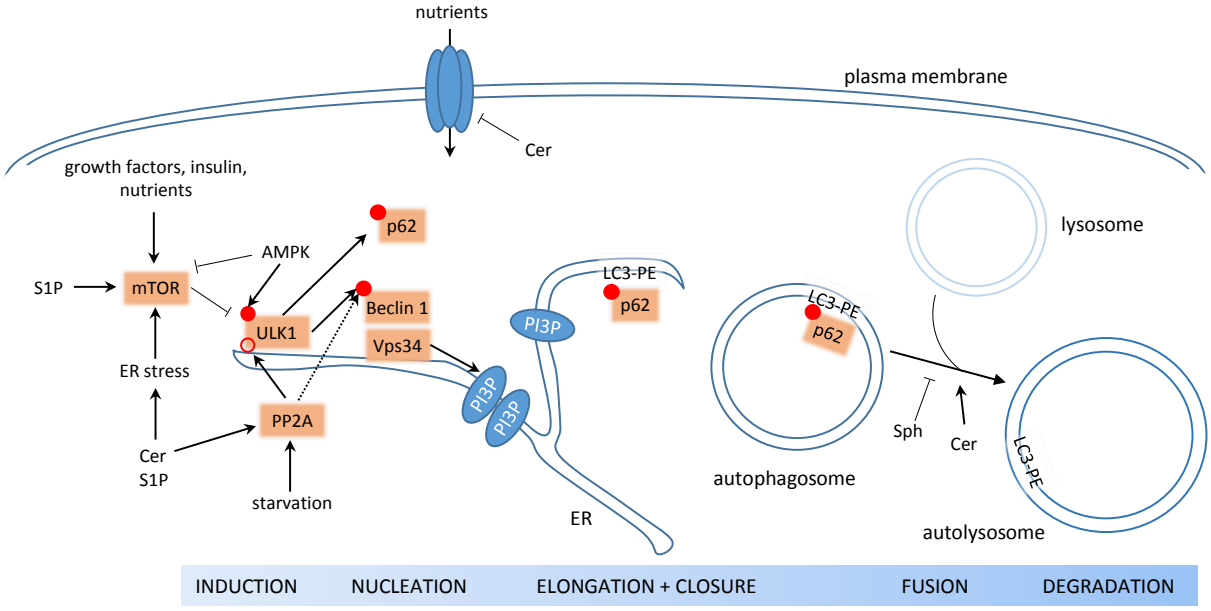

Figure 2 Stages of autophagy and their regulation
Sphingolipids influence autophagy regulation and progression on multiple levels. Cer – ceramide, S1P – sphingosine-1-phosphate, Sph – sphingosine, ER – endoplasmic reticulum, mTOR – mammalian target of rapamycin, AMPK - adenosine monophosphate-activated protein kinase, ULK - unc-51-like kinase, PP2A – protein phosphatase 2A, Vps - vacuolar protein sorting, LC3-PE - Microtubule-associated protein 1 light chain 3 conjugated with phosphatidylethanolamine. Adapted from Harvald *et al.* 2015.

Sphingolipids are known to regulate autophagy at various stages. S1P and C1P have been reported to induce autophagy (Taniguchi *et al.* 2012; Lavieu *et al.* 2006; Gagliostro *et al.* 2012). Ceramides, however, can influence autophagic processes in diametrically opposed ways,

depending on the setting. For example, ceramides activate AMPK indirectly by reducing the abundance of nutrients (Guenther *et al.* 2008). Additionally, ceramides have also been shown to promote PP2A activity (Dobrowsky *et al.* 1993; Oaks and Ogretmen 2014). Studies using acid sphingomyelinase inhibitors showed, that mainly C18 ceramides located in the endoplasmic reticulum ER activate PP2A and thereby initiate autophagic processes. There is evidence that ceramides also promote the fusion of autophagosomes and lysosomes (Harvald *et al.* 2015). The involvement of acid sphingomyelinase in the analogous process of phagosome-lysosome fusion events has also been shown (Schramm *et al.* 2008).

1.2.3 Acid sphingomyelinase

1.2.3.1 Structure, Localization, Activation

The ASM (human; in mice: Asm) is classified under the enzyme commission number 3.1.4.12, identifying it as a phosphodiesterase. The human sphingomyelin phosphodiesterase 1 gene (*SMPD1*; in mice: *Smpd1*), which comprises 5 – 6 kbp, encodes the 629 amino acids of the protein. The ASM can be differentially modified post-translationally in the Golgi, generating a secretory and a lysosomal protein. Apart from their localization, these two forms of the ASM are mainly distinguished by their N-terminal processing and glycosylation patterns (Schissel *et al.* 1998a). While the lysosomal enzyme contains N-linked oligomannose groups, allowing for lysosomal targeting via the mannose-6-phosphate receptor, the secreted form of the ASM shows a complex glycosylation pattern (Schissel *et al.* 1998b). Additionally, there are also differences in processing the length of the protein: the secreted form initiates at histidine 60, whereas the lysosomal ASM is cleaved at glycine 66 (Schissel *et al.* 1998b). The enzyme exhibits phospholipase C activity – hydrolyzing sphingomyelin to ceramide and releasing the phosphocholine headgroup. The ASM was first isolated from rat tissue in 1966 (Kanfer *et al.* 1966). Thereafter, it was readily identified as the cause of Niemann-Pick disease type A and B, which is characterized by the massive accumulation of sphingomyelin in a range of organs (Brady *et al.* 1966).

The crystal structures of the human as well as the murine protein have only been solved recently (Zhou *et al.* 2016; Gorelik *et al.* 2016). The human and murine genes show more than 80 % sequence similarity, leading to proteins with likewise very similar structures. The ASM is a multi-domain enzyme. The N-terminal domain is homologous to saposins, a proline-rich

linker forms a hinge region to the catalytic domain of the enzyme and the C-terminal domain. Even though the internal saposin domain renders ASM independent of sphingolipid activator proteins, SAP-C has been reported to increase its activity in vitro in the absence of detergents (Linke *et al.* 2001). Earlier reports however have shown a decrease in the activity of purified ASM upon addition of various saposins (Tayama *et al.* 1993). Crystal structures, visualizing the interaction of the enzyme with membranes, revealed the mechanism of how the saposin domain makes the headgroup of sphingomyelin accessible to the active site of the enzyme (Xiong *et al.* 2016). Conserved amino acids within the active site stabilize the substrate as well as the leaving group after cleavage of the phosphodiester bond. The mechanism of that cleavage relies on the action of two zinc ions, making sphingomyelin a metallophosphoesterase. The zinc ions interact with sphingomyelin's phosphate group and activate a water molecule to enable the nucleophilic attack on the phosphate atom (Zhou *et al.* 2016).

The enzyme is protected from degradation by lysosomal hydrolases, especially cathepsins, by two main features: membrane association and glycosylation. N-glycosylations on the side of the enzyme that is exposed to the lumen of the lysosome, prevent access of hydrolyzing enzymes. Whereas the other side of the ASM is inaccessible to degrading enzymes due to its association with the membrane of intraluminal vesicles (Kölzer *et al.* 2004). Positively charged amino acids on the membrane-facing part of the enzyme tightly interact with the negatively charged headgroups of the membrane lipids, which are enriched in the lysosome, e. g. bis(monoacylglycero)phosphate (BMP).

The acid sphingomyelinase derives its name from its optimal catalyzing efficiency at low pH, as is common for lysosomal enzymes. However, it has also been shown to work at physiologic pH under certain conditions (Schissel *et al.* 1998a; Schissel *et al.* 1998b). Apart from pH there are several additional factors influencing the enzymatic activity of the ASM. For one, the two zinc ions in the active site are indispensable for the catalytic process. As the secretory form of the ASM does not encounter zinc ions before its secretion via the secretory pathway, it requires the presence of extracellular zinc ions to be active (Schissel *et al.* 1996; Schissel *et al.* 1998a).

The C-terminal cysteine residue of the ASM has been reported as being involved in complexing a zinc ion within the active site. Thereby, the cysteine renders the ion less capable of activating

the water molecule, whose nucleophilic attack leads to the cleavage of sphingomyelin's phosphodiester bond (Qiu *et al.* 2003). It was shown that C-terminal proteolytic processing, which occurs within the endolysosomal compartment, enhances the activity of the ASM (Jenkins *et al.* 2011). Removal of the free thiol group of this terminal cysteine – be it via deletion, dimerization, modification or substitution – enhances the enzyme's activity (Qiu *et al.* 2003; Zhang and Li 2010). One such stimulus-induced activation of ASM was reported as occurring in response to TNFα-receptor activation. This activation of the ASM involved the removal of a C-terminal portion of the enzyme by caspase 8 within the lysosomal compartment (Edelmann *et al.* 2011).

The ASM can also be activated via the protein kinase C delta (PKCδ)-mediated phosphorylation at serine residue 508 (Zeidan and Hannun 2007). In addition, the enzymatic activity is increased by the presence of BMP and other anionic lipids in the membrane (Linke *et al.* 2001). BMP and phosphatidylinositol are especially enriched in the intraluminal vesicles of lysosomes, where ASM is active (Kobayashi *et al.* 1998).

There is a wealth of evidence supporting a general role of the ASM in cellular stress responses. A wide variety of stress-related triggers can lead not only to the activation of the ASM but also to its translocation to the outer leaflet of the plasma membrane. This occurs via the fusion of lysosomes with the plasma membrane. Such activating stimuli include but are not limited to viral and bacterial infections, treatment with anti-cancer agents, UV-light and stimulation of a range of receptors such as CD95 and FcrγRII (Abdel Shakor *et al.* 2004; Avota *et al.* 2011; Charruyer *et al.* 2005; Cremesti *et al.* 2001; Dumitru and Gulbins 2006; Grassmé *et al.* 2003; Grassmé *et al.* 2005; Hauck *et al.* 2000; Rotolo *et al.* 2005).

The conversion of sphingomyelin to ceramide in the outer leaflet of the plasma membrane is the foundation for the majority of ASM-mediated effects. The associated changes in membrane fluidity result in the segregation of proteins, thereby modulating their interactions. Often, this leads to an amplification of the original signal, exacerbating the response. (Stancevic and Kolesnick 2010).

1.2.3.2 Ceramide-enriched membrane domains

The plasma membrane is not a uniform mixture of lipids, but shows differences in composition not only between inner and outer leaflet, but also in the lateral distribution of lipids within a

monolayer. The exoplasmic side of the membrane is particularly rich in sphingomyelin, glycosphingolipids, and cholesterol which segregate into domains separate from glycerophospholipids (Simons and Ikonen 1997). Whereas glycerophospholipids are predominantly in liquid-disordered states, an abundance of sphingomyelin and cholesterol increases the rigidity and order of the membrane, inducing a so-called liquid-ordered phase (Quinn and Wolf 2009). Acyl chain length and saturation in sphingolipids as well as the rigid sterol ring system of cholesterol contribute to these properties, leading to the formation of so-called rafts of highly ordered lipids. These rafts do not only differ in their lipid make-up but are also enriched in certain proteins, such as proteins anchored to the membrane by glycosylphosphatidylinositol (GPI) or saturated fatty acid moieties, but also unlipidated proteins, while excluding for example prenylated proteins (Sezgin *et al.* 2017). This is – at least in part – due to the differences in the properties of the membrane, namely its thickness and fluidity.

Upon activation and translocation of ASM to the outer leaflet of the plasma membrane, it hydrolyses sphingomyelin to ceramide. Ceramide molecules tend to self-associate, aggregate and ultimately displace cholesterol from these lipid domains. This entails a further decrease in membrane fluidity which thereby limits the lateral movement of lipids and proteins (Lingwood and Simons 2010). Essentially, this entraps proteins within these areas of the membrane while limiting the “diffusion” of other proteins into these domains, thus modulating protein-protein interactions. Small ceramide-enriched microdomains are prone to coalesce into larger domains, eventually forming large platforms that are detectable by light microscopy (Kolesnick *et al.* 2000). Within these large areas, alterations occur as to whether and how receptors and co-receptors or inhibitory molecules come into contact or how they interact with ligands. This influences not only the duration and strength of the interactions as well as cross-reactivities but possibly also the association of molecules with these signaling complexes on the cytoplasmic side of the membrane (Grassmé *et al.* 2003). This already implies the conceivably huge impact ASM can have on signaling. Thus, it comes as no surprise that a host of proteins and their downstream effects are influenced by ASM activation and translocation and its subsequent modification of membrane properties.

Apart from altering membrane properties the generation of ceramide can also exert effects by direct interaction with a number of molecules: Cathepsin D (Heinrich *et al.* 1999),

phospholipase A2 (PLA2) (Huwiler *et al.* 2000), kinase suppressor of Ras (Zhang *et al.* 1997), ceramide-activated protein serine-threonine phosphatases (CAPP) (Dobrowsky and Hannun 1992), Protein kinase C (PKC) (Huwiler *et al.* 1998; Müller *et al.* 1995), potassium channel Kv1.3 and calcium release-activated calcium channels (Gulbins *et al.* 1997; Lepple-Wienhues *et al.* 1999; Samapati *et al.*). Furthermore, it was shown that ceramide molecules come together in a way that allows them to form channels. This was demonstrated to occur in the outer mitochondrial membrane, suggesting a possible contribution to the induction of apoptosis via cytochrome c release (Siskind and Colombini 2000).

1.2.3.3 ASM in disease

Given the impact the action of the ASM can have on cellular signaling processes, it is only to be expected that a dysregulation of the enzyme can have a variety of effects. Depending on the cell type affected and the accompanying circumstances, these effects can lead to various pathologic manifestations. However, as ASM is activated by a large number of different stimuli, an alteration in the enzyme's activity and all subsequent effects may be secondary to previously manifest pathologies. In a wide array of diseases ASM activity has been shown to be elevated: atherosclerosis (Devlin *et al.* 2008; Kinnunen and Holopainen 2002), diabetes mellitus type 2 (Górska *et al.* 2003; Herschkovitz *et al.* 2007), liver diseases like Wilson's disease (Lang *et al.* 2007), hepatic fibrosis (Quillin *et al.* 2015), chronic hepatitis C and non-alcoholic fatty liver disease (Grammatikos *et al.* 2014), pulmonary diseases (Von Bismarck *et al.* 2008), alcoholism (Reichel *et al.* 2010), status epilepticus (Mikati *et al.* 2008), Alzheimer's (He *et al.* 2010), and major depressive disorder (MDD) (Kornhuber *et al.* 2005; Gulbins *et al.* 2013). In some cases significantly increased ceramide levels have been reported: inflammatory bowel disease (Bauer *et al.* 2009), diabetes (Galadari *et al.* 2013; Straczkowski *et al.* 2007), and cystic fibrosis (Becker *et al.* 2010; Ziobro *et al.* 2013). It needs to be determined for each disease, whether the increase in ASM activity is a contributing factor to the development of the disease or simply one of its effects. While it is less likely that the ASM is the sole source for many of the mentioned ailments, it is plausible to assume that it can exacerbate physiologic responses, affecting severity and/or onset of pathologic manifestations.

Ultimately, therapeutic interventions are the goal of any such study. Interestingly enough, there are already drugs on the market that have been in use for decades with proven effects,

though their basic mechanism may have been misunderstood all this time. Tricyclic antidepressants have been used since the 1950s. They were thought to exert their antidepressant effects due to their action as serotonin reuptake inhibitors (Horn 1980). More recently they have been found to act in a different way as well. Being cationic amphiphilic drugs (CADs) they are being trapped in lysosomes upon protonation. Subsequently, their hydrophilic tail inserts into the membrane while the positively charged headgroup significantly alters the charge distribution of the otherwise predominantly anionic lysosomal membrane (Kornhuber *et al.* 2011). Consequently, lipid hydrolases that bind to the membranes via electrostatic interactions (including ASM) are displaced from the membrane, making them vulnerable to degradation by lysosomal enzymes (Hurwitz *et al.* 1994; Kölzer *et al.* 2004). In this way these drugs as well as other CADs act as functional inhibitors of the ASM (FIASMAs). It has been postulated that it is this inhibition and its downstream effects that ultimately help relieve symptoms of depression (Kornhuber *et al.* 2014; Gulbins *et al.* 2018). The potential for treatment of other ASM-associated diseases is being explored (Gulbins *et al.* 2018; Becker *et al.* 2018; Beckmann 2017; Beckmann *et al.* 2014).

1.2.3.4 ASM transgenic mice

It is common to use animal models to investigate the effects of alterations of certain physiologic processes. The mouse models for defects in ASM activity have been in use for more than 20 years (Horinouchi *et al.* 1995). A transgenic mouse to look into the effects of heightened Asm activity, however, has only been developed some years ago. So far these mice have only been employed in a handful of studies with focus on a few select diseases: depression, cystic fibrosis, and alcoholism (Gulbins *et al.* 2013; Grassmé *et al.* 2017; Müller *et al.* 2017). In 2013 it was shown that mice overexpressing ASM are impaired in adult neurogenesis, neuronal maturation and survival. Increased ceramide levels in the hippocampus correlated with depression-like behavior. The inhibition of ASM using FIASMAs resulted in a normalization of ceramide levels and the behavior of the mice (Gulbins *et al.* 2013; Kornhuber *et al.* 2014). These effects are mediated by an increase in ceramide within the ER and its activation of positive regulators of autophagy (Gulbins *et al.* 2018). The cerebrospinal fluid of these mice showed elevated ASM levels, indicating an increased secretion of the enzyme as well (Mühle *et al.* 2013). ASM hyperactivity in mice has also been

implicated in modulation of effects secondary to depression, i. e. alcoholism (Müller *et al.* 2017).

In a study on cystic fibrosis, mice overexpressing Asm or deficient for acid ceramidase (Ac) were employed as controls, mimicking the accumulation of ceramide in CF mice. As such, they displayed a pulmonary phenotype similar to Cftr-deficient mice. They also showed a comparable imbalance in ceramide and sphingosine levels. Ceramide accumulated particularly in bronchial epithelial cells, while sphingosine levels were markedly reduced, which was associated with an increased susceptibility to bacterial infections (Grassmé *et al.* 2017).

As ASM hyperactivity has been associated with an even wider variety of diseases, these Asm overexpressing mice may be a promising model for the study of further pathologies.

2 AIM OF THE STUDY

Most ASM-related diseases have been solely studied under the aspect of activity reduction by use of knock-out mice or pharmacologic inhibitors. This study aims to describe a transgenic mouse model in which the Asm is constitutively overexpressed, to lay the foundation for further studies. The focus here is on the characterization of murine lungs with exacerbated Asm activity. Comparative analyzes between wild-type mice and transgenic mice with respect to enzyme activity, lipid composition, organ morphology and inflammatory values aim to gauge the baseline phenotype that the overexpression of the Asm gene entails. The ultimate goal is to ascertain the suitability of these mice for studies of Asm-related diseases.
As such these mice would allow for investigations of the wide spectrum of diseases that the ASM seems to affect. A variety of pathologies in humans are associated with increased ASM serum levels or enzyme activities (Devlin *et al.* 2008; Herschkovitz *et al.* 2007; Lang *et al.* 2007; Quillin *et al.* 2015; He *et al.* 2010). This includes diseases of the nervous system, where sphingomyelin is especially abundant, as well as diseases affecting other organs, such as liver, joints, and intestine.

3 MATERIALS AND METHODS

3.1 Materials

3.1.1 Chemicals

Acetic acid (100 %)	Merck KGaA, Darmstadt, Germany
Acrylamide	Carl-Roth GmbH & Co, Karlsruhe, Germany
Ammonium persulfate (APS)	Carl-Roth GmbH & Co, Karlsruhe, Germany
Aprotinin	Roche Deutschland Holding GmbH, Freiburg, Germany
BODIPY™ FL C_{12}-sphingomyelin (N-(4,4-difluoro-5,7-dimethyl-4-bora-3a,4a-diaza-s-indacene-3-dodecanoyl) sphingosyl phosphocholine	Thermo Fisher Scientific, Waltham, MA, USA
Bovine serum albumin (BSA), fatty acid free	Sigma-Aldrich Chemie GmbH, Steinheim, Germany
Protein Assay Dye Reagent Concentrate	Biorad Laboratories GmbH, München, Germany
Bromphenol blue	Sigma-Aldrich Chemie GmbH, Steinheim, Germany
Calcium chloride (≥ 99 %)	Carl-Roth GmbH & Co, Karlsruhe, Germany
Chloroform	AppliChem GmbH, Darmstadt, Germany
Dimethylsulfoxide	Sigma-Aldrich Chemie GmbH, Steinheim, Germany
Dipotassium hydrogen phosphate	Carl-Roth GmbH & Co, Karlsruhe, Germany
Disodium hydrogen phosphate	Merck KGaA, Darmstadt, Germany
Dithiothreitol	Carl-Roth GmbH & Co, Karlsruhe, Germany
Eosin	Carl-Roth GmbH & Co, Karlsruhe, Germany
Ethanol (absolute, anhydrous)	Diagonal GmbH & Co. KG, Münster, Germany
Ethyl acetate	Diagonal GmbH & Co. KG, Münster, Germany
Fetal calf serum	Gibco/Invitrogen, Karlsruhe , Germany
Hematoxylin	Carl-Roth GmbH & Co, Karlsruhe, Germany
HEPES	Carl-Roth GmbH & Co, Karlsruhe, Germany
Hydrochloric acid (fuming, 37 %)	Sigma-Aldrich Chemie GmbH, Steinheim, Germany

Isopropanol	Sigma-Aldrich Chemie GmbH, Steinheim, Germany
Leupeptin	Becton, Dickinson GmbH, Heidelberg, Germany
Liquid Nitrogen	AIR LIQUIDE Medical GmbH, Düsseldorf, Germany
Magnesium chloride hexahydrate (≥ 99 % p.a.)	Carl-Roth GmbH & Co, Karlsruhe, Germany
Magnesium sulfate heptahydrate (≥ 99 %)	Sigma-Aldrich Chemie GmbH, Steinheim, Germany
β-Mercaptoethanol	Sigma-Aldrich Chemie GmbH, Steinheim, Germany
Methanol (≥ 99.8 %)	Diagonal GmbH & Co. KG, Münster, Germany
Monopotassium phosphate	Merck KGaA, Darmstadt, Germany
NBD-C_{12}-ceramide, N-[(1S,2R,3E)-2-hydroxy-1-(hydroxymethyl)-3-heptadecen-1-yl]-12-[(7-nitro-2,1,3-benzoxadiazol-4-l)amino]-dodecanamide	Thermo Fisher Scientific, Waltham, MA, USA
NP-40 (Igepal)	Sigma-Aldrich Chemie GmbH, Steinheim, Germany
Paraformaldehyde (powder, 95 %)	Sigma-Aldrich Chemie GmbH, Steinheim, Germany
Paraplast	Leica Mikrosysteme Vertrieb GmbH, Wetzlar, Germany
Pepsin Solution Digest-All	Thermo Fisher Scientific, Waltham, MA, USA
Polyoxyethyle glycol sorbitan monolaurate (Tween20)	Sigma-Aldrich Chemie GmbH, Steinheim, Germany
Potassium chloride (≥ 99 %)	Carl-Roth GmbH & Co KG, Karlsruhe, Germany
Sodium chloride (≥ 99,5 %)	Carl-Roth GmbH & Co KG, Karlsruhe, Germany
Sodium hydroxide	Sigma-Aldrich Chemie GmbH, Steinheim, Germany
Sodium dihydrogen phosphate	Merck KGaA, Darmstadt, Germany
Starting Block TBS Blocking Solution	Thermo Fisher Scientific, Waltham, MA, USA
Xylene (mixture of isomers)	Diagonal GmbH & Co. KG, Münster, Germany

3.1.2 Antibodies & kits

HRP-coupled anti-beta-actin	SantaCruz Biotechnology, Inc., Dallas, TX, USA
anti-rabbit HRP-coupled IgG	SantaCruz Biotechnology, Inc., Dallas, TX, USA
anti-rabbit AP-coupled IgG	SantaCruz Biotechnology, Inc., Dallas, TX, USA
Cy™3 AffiniPure $F(ab')_2$ fragment donkey anti-mouse IgM, µ chain	Jackson ImmunoResearch Europe Ltd., Suffolk, UK
Cy™3 AffiniPure $F(ab')_2$ fragment donkey anti-rat IgG (H+L)	Jackson ImmunoResearch Europe Ltd., Suffolk, UK
mouse anti-ceramide IgM clone S58-9, serum-free supernatant	Glycobiotech GmbH, Kükels, Germany
rat anti-mouse Gr1 (Ly6G, Ly6C) IgG, clone RB6-8C5 (RUO)	Becton Dickinson Biosciences, Heidelberg, Germany
rabbit anti-mouse LC3B, polyclonal	Cell Signaling Technology, Danvers, MA, USA
rabbit anti-mouse phospho-beclin-1 (Ser15) IgG, clone D4B7R	Cell Signaling Technology, Danvers, MA, USA
rabbit anti-phospho-mTOR (Ser2448) IgG, clone D9C2	Cell Signaling Technology, Danvers, MA, USA
rabbit anti-mTOR, polyclonal	Cell Signaling Technology, Danvers, MA, USA
rabbit anti-phospho-PP2A (Tyr307) IgG, polyclonal	R&D Systems Inc., Minneapolis, MN, USA
rabbit anti-PP2A alpha+beta IgG, clone E155	Abcam plc, Cambridge, UK
rabbit anti-p62, polyclonal	Sigma-Aldrich Chemie GmbH, Steinheim, Germany
rabbit anti-ULK1 IgG, clone D8H5	Cell Signaling Technology, Danvers, MA, USA
rabbit anti-phospho-ULK1 (Ser555) IgG, clone D1H4	Cell Signaling Technology, Danvers, MA, USA
rabbit anti-phospho-ULK1 (Ser757), polyclonal	Cell Signaling Technology, Danvers, MA, USA

ECL prime system	GE Healthcare Europe GmbH, Freiburg, Germany
IL-1β (mouse) Quantikine ELISA	R&D Systems Inc., Minneapolis, MN, USA
IL-6 (mouse) Quantikine ELISA	R&D Systems Inc., Minneapolis, MN, USA
TNFα (mouse) Quantikine ELISA	R&D Systems Inc., Minneapolis, MN, USA
KC (mouse) Quantikine ELISA	R&D Systems Inc., Minneapolis, MN, USA
Trichrome Stain (Masson) Kit	Sigma-Aldrich Chemie GmbH, Steinheim, Germany
Soluble Collagen Assay Sircol™	Biocolor Ltd, Carrickfergus, UK

3.1.3 Buffers and solutions

Ac/Asm assay buffer	250 mM sodium acetate 0,1 % NP-40 100 µM $ZnCl_2$ (Asm) pH 4,5 (Ac) or pH 5,0 (Asm)
Ac/Asm lysis buffer	250 mM sodium acetate 1 % NP-40 pH 4,5 (Ac) or pH 5,0 (Asm)
Ac substrate solution	100 pmol NBD-ceramide in 180 µl Ac assaybuffer
Asm substrate solution	100 pmol BODIPY-sphingomyelin in 180 µl Asm assaybuffer
HEPES/Saline (HS) (10x)	200 mM HEPES 1,32 M NaCl 10 M $CaCl_2$ 7 mM $MgCl_2$ 8 mM $MgSO_4$ 54 mM KCl
Mowiol	20-25 % Mowiol-488 2,5 % Dabco
Paraformaldehyde (PFA), 4 %	4 % PFA 1 x PBS pH 7,2 – 7,4 adjusted with HCl and NaOH
Phosphate buffered saline (PBS)	137 mM NaCl 2,7 mM KCl 10 mM $Na_2HPO_4 \bullet 2\ H_20$

	2 mM KH_2PO_4
	pH adjusted with HCl and NaOH to 7,2 - 7,4
Reducing SDS sample buffer (5x)	250 mM Tris pH 6.8
	20 % glycerine
	4 % SDS
	8 % ß-mercaptoethanol
	0,2 % bromphenol blue
SDS Running buffer	25 mM Tris
	192 mM glycine
	0,1 % SDS
TN3 lysis buffer	125 mM NaCl
	10 mM EDTA
	25 mM Tris pH 7,4
	10mM $Na_4P_2O_7$
	3 % NP40
	10 µg/ml aprotinin and leupeptin
	10 mM sodium orthovanadate, freshly prepared

3.1.4 Consumables

Cell culture flasks	Sarstedt AG & Co, Nümbrecht, Germany
Centrifuge tubes (15 mL, 50 mL)	Greiner Bio-One GmbH, Frickenhausen, Germany
Coverglasses	
18 x 18 mm	Engelbrecht GmbH, Wien, Austria
24 x 50 mm	Carl-Roth GmbH & Co, Karlsruhe, Germany
Cuvettes	Sarstedt AG & Co, Nümbrecht, Germany
Embedding cassettes	Carl-Roth GmbH & Co, Karlsruhe, Germany
Hybond ECL nitrocellulose membrane	GE Healthcare Europe GmbH, Freiburg, Germany
Hypodermic needle	Becton Dickinson GmbH, Heidelberg, Germany
Microscopic slides	Langenbringen Labor- und Medizintechnik, Emmendingen, Germany
Microtiter plates	Sarstedt AG & Co, Nümbrecht, Germany
Needles (different gauges)	Becton Dickinson GmbH, Heidelberg, Germany
Pipettes (5 mL, 10 mL, 25 mL)	Greiner Bio-One, Frickenhausen, Germany

Reaction tubes, 1,5 mL	Sarstedt AG & Co, Nümbrecht, Germany
Protein LoBind tubes, 1,5 ml	Eppendorf AG, Hamburg, Germany
Screw cap graduated tubes, 1,5 ml	STARLAB Intl. Gmbh, Hamburg, Germany
Syringes	
- Insulin syringe	Becton Dickinson GmbH, Heidelberg, Germany
- Luer-lock 1 mL syringe	Becton Dickinson GmbH, Heidelberg, Germany
- Rubber- and lubricant free	Sigma-Aldrich Chemie GmbH, Steinheim, Germany
Thin layer chromatography (TLC) Silica G60 plates	Merck KGaA, Darmstadt, Germany
X-Ray films	GE Healthcare Europe GmbH, Freiburg, Germany

3.1.5 Instruments/equipment

Centrifuges	
- 5417 R	Eppendorf AG, Hamburg, Germany
- Heraeus 3SR+ multifuge	Thermo Fisher Scientific, Waltham, MA, USA
Confocal fluorescence microscope (TCS-SP5)	Leica Mikrosysteme Vertrieb GmbH, Wetzlar, Germany
Developer machine	Thermo Fisher Scientific, Waltham, MA, USA
Freezers	Sanyo Electric Co, Osaka, Japan
- 80 °C, ultra-low MDF-U54V	Liebherr-International Deutschland GmbH, Biberach,
- 20 °C, Premium NoFrost	Deuschland
Fridge (4 °C, Premium BioFresh)	Liebherr-International Deutschland GmbH, Biberach, Germany
Glasswares (beakers, cylinders, flasks)	DURAN Group GmbH, Wertheim, Germany
Incubator	Binder GmbH, Tuttlingen, Germany
Infrared lamp	Philips Consumer Lifestyle B.V., Drachten, The Netherlands
Magnetic stirrer (M21)	Intern. Laborat. App GmbH, Dottingen, Germany
Mass spectrometer (Q-TOF 6530)	Agilent Technologies, Waldbronn, Germany
Mechanical shaker (Rotamax120)	Heidolph Instruments GmbH & Co. KG, Schwabach, Germany
pH Meter (HI9025)	Hanna instruments, Woonsocket, RI, USA
Pipettes (different sizes)	Nichiryo CO., Ltd., Saitama, Japan

Pipettor (pipetus-akku)	Hirschmann Laborgeräte GmbH und Co. KG, Eberstadt, Germany
Rotary microtome (Microm HM 355S)	Thermo Scientific, Waltham, MA, USA
Spectrophotometer	Eppendorf AG, Hamburg, Germany
Vacuum Concentrator (SpeedVac)	Thermo Fisher Scientific, Waltham, MA, USA
Thermomixer	Eppendorf AG, Hamburg, Germany
Typhoon FLA 9500	GE Healthcare Europe GmbH, Freiburg, Germany
Ultrasonic bath (sonorex RK 102 H)	BANDELIN electronic GmbH & Co. KG, Berlin, Germany
Vortexer (Reax 2000)	Heidolph Instruments GmbH & Co. KG, Schwabach, Germany
Water bath (1o12)	GFL Gesellschaft für Labortechnik mbH, Burgwedel, Germany
Branson Bransonic® CPXH Digital Bath 5800	Emerson Electric Co, Saint Louis, MO, USA

3.1.6 Software

GraphPad Prism (5.01)	GraphPad Software, La Jolla, CA, USA
ImageQuant	GE Healthcare Europe GmbH, Freiburg, Germany
Leica Application Suite – Advanced Fluorescence (2.61)	Leica Mikrosysteme Vertrieb GmbH, Wetzlar, Germany
MassHunter Software	Agilent Technologies, Waldbronn, Germany
Microsoft Office (2016)	Microsoft Corporation, Redmond, WA, USA

3.2 Methods

3.2.1 Animal husbandry

Mice were kept in the animal facility of the University Hospital Essen according to the Federations of European Laboratory Animal Science Association's (FELASA) guidelines. They were housed under pathogen-free conditions and subject to a 12h/12h light/dark cycle. The animals were given *ad libitum* access to food and water.

3.2.2 Generation of the transgenic mouse model

The Asm-transgenic mouse strain (tAsm) was generated by genOway, France. They developed a "Quick Knock-In™" targeting vector (Figure 3) which is inserted via homologous recombination into the previously disrupted hypoxanthine phosphoribosyl-transferase (*Hprt*) gene locus, by which means successful recombination events can be screened for. The *Hprt* gene encodes an enzyme of the purine nucleotide salvage pathway. Cells lacking this gene will die, if grown in medium that does not allow for *de novo* nucleotide synthesis (HAT medium, containing hypoxanthine, aminopterin, and thymidine). Cells containing the recombined *Hprt* locus and therefore also the Asm transgene, can survive in HAT medium by using the salvage pathway to generate purine bases.

The inserted Asm gene (*Smpd1* cDNA) is expressed under the control of the ubiquitous CAG promoter (a fusion of the CMV immediate early enhancer and chicken β-actin promoter). A loxP flanked STOP cassette between the promoter and the Asm allows for conditional expression of the Asm by crossing the tAsm mice with a Cre recombinase expressing mouse strain. Depending on the promoter regulating Cre expression time- or tissue-specific Asm expression can be achieved. The tAsm mice are maintained on a C57Bl/6 background. The target vector was inserted into E14 embryonic stem cells derived from 129P2/Ola mice. Successfully recombined cells were used to create chimeric mice by way of C57BL/6 blastocyst injection. Transgenic mice were backcrossed to C57BL/6 mice for at least 5 generations. To achieve expression of the transgene the mice were mated with E2a-Cre transgenic C57BL/6 mice, expressing Cre recombinase under the constitutively active E2a promoter.

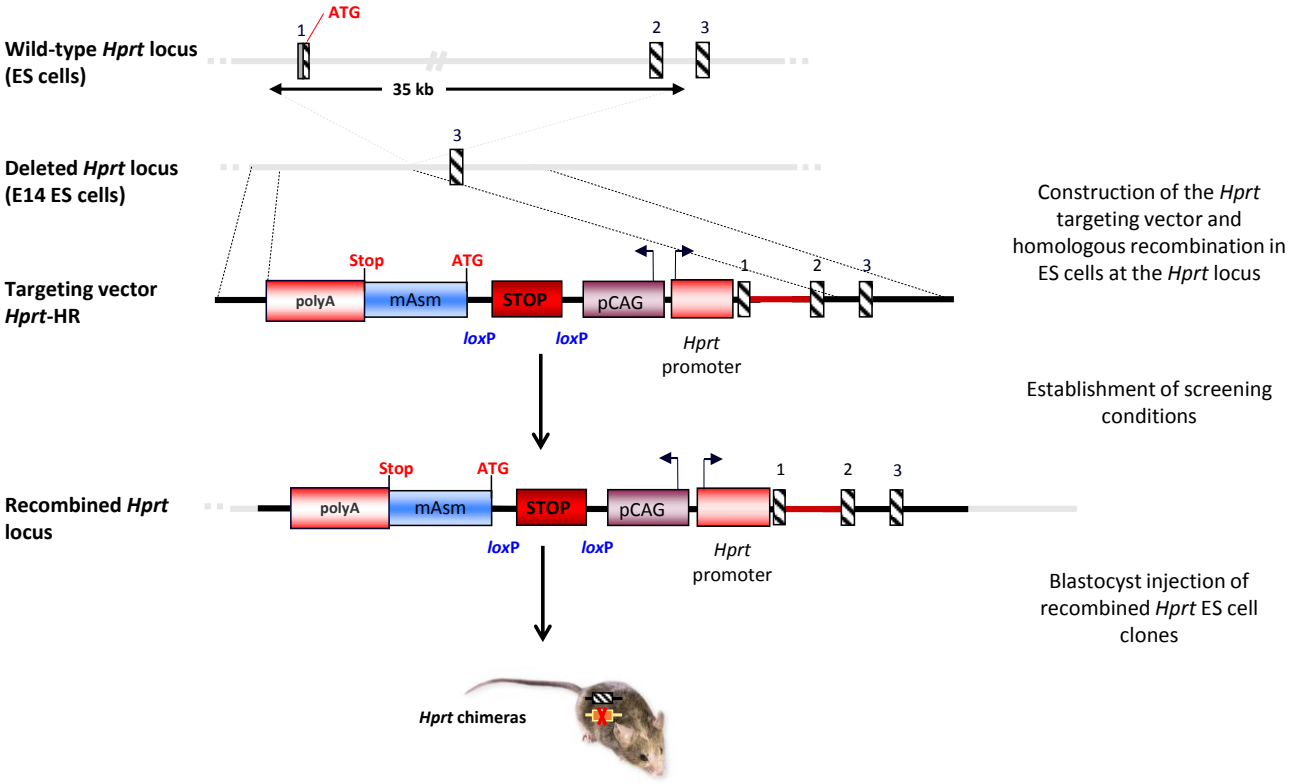

Figure 3 *Hprt* "Quick Knock-in™"approach, genOway
The makeup of the targeting vector as well as the sites of insertion into the partially deleted *Hprt* locus of embryonic stem cells are shown. The depiction is not to scale. Striped boxes represent exons, lines represent introns. ES cells = embryonic stem cells; *Hprt* = gene encoding hypoxanthine phosphoribosyltransferase; polyA = polyA tail encoding sequence; mAsm = cDNA sequence of the murine Asm gene, *Smpd1*; STOP = STOP cassette, loxP = Cre recombinase target sequence; pCAG = CMV immediate early enhancer / chicken β-actin promoter. Image adapted from genOway's breeding reports.

3.2.3 Acid sphingomyelinase/ acid ceramidase activity assays

The activities of the acid sphingomyelinase and acid ceramidase were ascertained using two analogous *in vitro* assays. Activities were determined in whole tissue lysates. To prepare lung tissue for lysis, the left lung was snap frozen in liquid nitrogen and pulverized using a pre-cooled mortar and pestle. About 10 mg of lung powder was sonicated in 150 µl lysis buffer (see section 3.1.3) twice for 10 seconds on ice using a tip sonicator. For the Asm activity assay the pH of the sodium acetate solution was adjusted to 5,0 whereas in the Ac activity assay a pH of 4,5 was used. Following protein quantification using the Bradford method (see section 3.2.7), lysates were adjusted to contain 0,5 µg or 20 µg of protein in 20 µl lysis buffer for the Asm and Ac activity assays, respectively. The fluorescently labeled substrates – BODIPY™ FL C_{12}-sphingomyelin as substrate for the Asm, NBD-C_{12}-ceramide for the Ac – were resuspended in their respective assay buffers (see section 3.1.3) to yield a substrate concentration of 100 pmol/180 µl. The 200 µl reaction mixtures comprised 20 µl of sample (0,5 µg or 20 µg of

protein) and 180 µl of the respective substrate solution (100 pmol substrate). The reactions proceeded at 37 °C in the dark with slight shaking at 300 rpm. After 1 h (Asm) or 3 h (Ac) the reactions were stopped by addition of methanol/chloroform (2:1, v/v) to extract the lipids from the reaction mixture. Upon centrifugation at maximum speed for 5 minutes, 100 µl of the lower phase were collected and dried using a vacuum centrifuge. Reconstitution of the resultant pellet in a small volume of chloroform/methanol (2:1, v/v) allowed for precise spotting on a thin layer chromatography (TLC) plate and subsequent separation of the lipids. The running chamber for the Asm assay contained chloroform/methanol (4:1, v/v), whereas the lipids from the Ac activity assay were separated using an ethyl acetate/acetic acid (100:1, v/v) running buffer. The fluorescence intensities on the dried plates were determined via a fluorescence laser scanner (Typhoon FLA 9500) and quantified using ImageQuant software. The read-out was used to deduce the amounts of reaction product and unconsumed substrate and to subsequently calculate the Asm or Ac activity.

3.2.4 Lipid quantification

Lipid quantification analyses were carried out by Fabian Schumacher at the University of Potsdam as published previously (Beckmann *et al.* 2018). Briefly, lung tissues were provided as powder of the left lung of about 10 mg per sample. Samples were homogenized and subjected to lipid extraction using methanol/chloroform (2:1, v/v). D7-sphingosine, C17-ceramide and C16-d31-sphingomyelin (all Avanti Polar Lipids, Alabaster, USA) were used as internal standards in the extraction solvent. The extracted lipids were evaporated to dryness and upon reconstitution subjected to mass spectrometric sphingolipid quantification. A 1200 series HPLC coupled to a quadrupole time-of-flight 6530 mass spectrometer was used to analyze ceramides and sphingomyelins. Sphingosine measurements were conducted using a 1260 Infinity HPLC system coupled to a 6490 triple quadrupole mass spectrometer. An electrospray ion source operating in the positive ion mode (ESI+) was interfaced with both instruments. Lipid analyses in MS/MS mode utilized the fragmentation of the respective precursor ions into the product ions: m/z 282.3 (for sphingosine), m/z 264.3 (for all ceramides) or m/z 184.07 (for all sphingomyelins). MassHunter software was employed to quantify the data.

3.2.5 Preparation of tissue sections

The tissue samples of the kidney, heart, and liver as well as the superior and middle lobes of the right lung were fixed in 4 % PFA for 36 h. Subsequently the tissues were dehydrated by incubation in an ascending graded ethanol-series of 50 % to 100 % over the course of the following days. The tissues were then cleared in two 30-minute xylene washes to be subsequently equilibrated in liquid paraffin baths at 65 °C in a three-step process. Finally the tissues were embedded in blocks of paraffin. These were cut at 6 µm per section using rotary microtome and mounted on SuperFrost Plus microscope slides. After drying the slides overnight at 50 °C they were stored at room temperature (RT) until commencement of a staining procedure.

To ready the slides for stainings of any kind they were deparaffinized in xylene and rehydrated in a descending graded ethanol-series of 100 % to 70 % to be finally washed in de-ionized water. The respective staining procedures were carried out directly after this preparation procedure.

3.2.6 Staining procedures

3.2.6.1 Hematoxylin and eosin stain (H&E stain)

Sections were prepared as described above and after rehydration the slides were stained for 5 minutes in acidic hemalum solution according to Mayer. The slides were blued for 15 minutes under flowing tap water. The counterstain was done with 0,1 % eosin in distilled water for 1 minute. Afterwards, the slides were dehydrated in two steps each in 96 % and 100 % ethanol and incubated in xylene thrice for 5 minutes to be subsequently embedded in Eukitt® mounting medium.

3.2.6.2 Masson’s trichrome stain

After preparing and rehydrating the sections as described in section 3.2.5, they were fixed in pre-warmed Bouin’s solution for 15 minutes at 56 °C. After cooling the slides with tap water and washing them for about 10 minutes until the yellow colour faded, they were stained using Sigma’s trichrome stain (Masson) kit. First, the sections were incubated for 5 minutes in freshly prepared iron hematoxylin solution (1:1, v/v, mixture of solutions A and B) according to Weigert. Afterwards, they were washed with tap water, rinsed with distilled water and counterstained for 5 minutes each with Biebrich scarlet-acid fuchsin solution, a 1:2 (v/v) mix

of phosphotungstic acid and phosphomolybdic acid solutions and an aniline blue solution. Finally, slides were incubated in 1 % acetic acid for 2 minutes, rinsed twice with distilled water and dehydrated and embedded as described in section 3.2.6.1.

3.2.6.3 Indirect immunofluorescence stainings

Stainings for ceramide and neutrophils both followed the same general procedure. Sections were prepared as described above (3.2.5) and subsequently treated with a pepsin solution for 30 minutes at 37 °C, thereby demasking epitopes and making them accessible for recognition by the respective antibody. This was followed by washing (PBS) and blocking (5 % FCS ± 0,05 % Tween20) steps, the latter to minimize any unspecific binding of the antibodies to the tissue. Antibodies were allowed to bind their respective antigens during an overnight incubation step at 4 °C. For this purpose, the neutrophil-specific rat anti-mouse Gr1 (Ly6G and Ly6C) antibody was employed at a dilution of 1:200, while the murine ceramide-specific antibody was diluted at a ratio of 1:100. After washing the slides thrice both primary antibodies were detected by secondary, Cy3-labeled antibodies (1:200 donkey anti-rat IgG or 1:500 donkey anti-mouse IgM) during 45-minute incubation periods at RT. Control slides lacking addition of primary antibodies to monitor unspecific binding of the secondary antibodies to the sections. Following three more washes, slides were mounted with Mowiol. Stainings were imaged using a Leica TCS SP5 confocal microscope and the corresponding Leica Application Suite Advanced Fluorescence software.

3.2.7 Western Blots

Whole tissue lysates were prepared by first pulverizing the left lungs under liquid nitrogen using mortar and pestle and subsequently lysing the powder in TN3 lysis buffer (see section 0) with the aid of a tip sonicator. Samples were sonicated twice for 10 seconds on ice. The protein content of the samples was determined using the Bradford method. Briefly, protein solutions of a known concentration prepared from a 10 mg/ml bovine serum albumin (BSA) stock solution as well as the samples were incubated for at least 5 minutes with Bradford reagent (1:5 dilution in water of Biorad's Protein Assay Dye Reagent Concentrate). Absorption of the resulting solutions at 595 nm was determined. As the absorption correlates with the protein content of the solution, a standard curve of the known protein concentrations is used to quantify the proteins in the samples.

Samples were incubated with 5x SDS-sample buffer for 5 minutes at 95 °C to denature and reduce the proteins. SDS-polyacrylamide gel electrophoresis (SDS-PAGE) was then employed to separate the proteins of each sample by size. Subsequent transferal of the proteins to a nitrocellulose membrane via an electric field (80 V for 2 h or 40 V overnight in a blotting chamber at 4 °C) made them accessible for antibody detection. Incubation with Pierce™ StartingBlock™ blocking buffer for 1 h at RT minimized unspecific binding of antibodies to the membrane. The membranes were incubated with primary antibodies overnight at 4 °C at the dilutions indicated in Table 1. Primary antibodies bound to their respective target protein bands on the membrane were visualized by labelling with a secondary, enzyme-coupled antibody for 1 h at RT (either anti-rabbit AP diluted 1:50 000 or anti-rabbit HRP diluted 1:10 000). These enzymes catalyze light-emitting reactions (chemiluminescence), which can be quite sensitively detected by X-ray films. Within its linear range the signal is directly proportional to the amount of antibody bound to the membrane and therefore to the amount of antigen (i.e. the protein of interest) present on the membrane. The amount of each protein was normalized to the amount of β-actin present in the sample, as determined using an HRP-coupled anti-actin antibody. Thus a semi-quantitative deduction of the amount of protein in a certain sample was possible.

Table 1 Antibodies used for Western Blot analyses
Specifications of antibodies used to detect autophagy-related proteins. All antibodies were raised in rabbits and can be detected by anti-rabbit secondary antibodies except actin, which is directly coupled to horseradish peroxidase.

Antigen	dilution	Expected size [kDa]	Cat.#, company
β-actin	1:50 000	43	Santa Cruz
p62	1:5 000	62	#P0067, Sigma-Aldrich
phospho-Beclin (Ser15)	1:1 000	60	#84966, CST
pI3K	1:1 000	100	#13857, CST
LC3B	1:5 000	16/18	#2775, CST
mTOR	1:1 000	289	#2972,CST
phospho-mTOR (Ser2448)	1:1 000	289	#5536, CST
PP2A	1:5 000	34	ab32104, abcam
phospho-PP2A (Tyr307)	1:200	34	#3989, R&D Systems
ULK1	1:1 000	150	#8054, CST
phospho-ULK1 (Ser555)	1:1 000	140-150	#5869, CST
phospho-ULK1 (Ser757)	1:1 000	140-150	#6888, CST

3.2.8 Enzyme-linked immunosorbent assays

Cytokines in the lung tissues were quantified using kits by R&D systems specific for IL-1β, IL-6, KC, TNFα, and GM-CSF. The assays were carried out according to the manufacturer's instructions. Lysates were prepared from roughly 15 mg of the pulverized left lungs of the mice. Samples were sonicated on ice (2 x 10") in 100 µl TN3 lysis buffer (see section 3.1.3) using a tip sonicator. 50 µl of each sample as well as of standards and controls were added to separate wells of microplate strips, which are pre-coated with antibodies specific for the respective cytokine, and incubated for 2 h at RT. Following washing steps to remove unbound lysate components, an enzyme-linked antibody directed against the cytokine in question was added to each well for another 2 h at RT. After removal of unbound antibody the substrate was added and converted by the enzyme to form a blue product. Addition of a stop solution after the 30-minute reaction period turned the reaction product yellow. The absorption at 450 nm is directly proportional to the amount of cytokine that was present in each sample. The standard curve is used to calculate the cytokine concentration in the samples. Cytokine amounts were normalized to the protein content of each sample as determined using the Bradford method (see section 3.2.7).

3.2.9 Cytokine array

R&D System's Proteome Profiler™ Array, Mouse Cytokine Array Panel A, was used to detect serum cytokines by following the manufacturer's instructions. Blood was collected from the tail vein of mice. The serum was obtained after a 30-minute coagulation period at RT and subsequent centrifugation of the sample. The clear supernatant (serum) was removed and stored at -20 °C before being assayed.

In short, the assay employs a nitrocellulose membrane upon which 40 different capture antibodies are spotted in duplicate to bind various cytokines present in the sample. Before adding the samples to the membrane, however, they were pre-incubated for 1 h at RT with a cocktail of biotinylated detection antibodies. The samples, now containing cytokines complexed with their respective detection antibodies, were incubated with the membrane at 4 °C overnight. Subsequently, the cytokines bound to the washed membrane were labeled with a streptavidin-HRP complex for 30 minutes. The generation of light by the action of HRP on its substrate can be detected using X-ray films. The localization of the spots are indicative of the cytokine bound by way of their capture antibody. The intensity of the light generated

corresponds to the amount of cytokine bound to the membrane. Thereby the levels of 40 cytokines per sample can be assessed.

3.2.10 Collagen quantification

The Sircol™ soluble collagen assay kit by Biocolor Ltd, UK, was used for collagen quantification. The assay was carried out as per the kit's manual. Fresh tissue samples (i.e. the inferior and post-caval lobes of the right lung) were diced, briefly washed with PBS and incubated with 1,2 ml 0,1 mg/ml pepsin in 0,5 M acetic acid at 4 °C overnight to extract collagen. An aliquot of the extracts was used to determine the protein content via the Bradford assay (see section 3.2.7). As recommended for samples containing low amounts of collagen, an isolation and concentration step was carried out before performing the actual quantification assay. To this end 1 ml of the cleared pepsin extract was first neutralized by adding 100 µl of the Acid Neutralizing Reagent contained in the kit and then incubated overnight at 4 °C with 200 µl of the kit's Isolation & Concentration Reagent. After centrifugation for 10 minutes at 15 000 x g and removal of 1 ml of the supernatant, the collagen pellet was resuspended in the remaining volume. Assuming that all the protein of the sample remained within the pellet, the volume corresponding to 60 µg of protein was removed from the collagen solution and used for the assay. The volume of the samples as well as the standards (0, 5, 10 and 15 µg rat collagen) was made up to 100 µl using 0,5 M acetic acid as a diluent. The quantification assay was commenced by staining collagen with the Sircol Dye Reagent in a 30-minute incubation step at RT and agitation at 300 rpm in a thermomix block. After another centrifugation for 10 minutes at 15 000 x g and removal of the supernatant dye solution, any unbound dye was washed from the reaction tube by gently layering 750 µl Acid-Salt Wash solution over the pellet. The samples were centrifuged under the same conditions once more and the resultant pellets were resuspended in 250 µl Alkali Reagent. Finally, 200 µl of the colored samples were transferred to a microwell plate and the absorptions at 555 nm were measured using a microplate reader. The collagen content of the samples could be inferred from the standard curve.

3.2.11 Statistics

Where applicable, data are presented as arithmetic means ± standard deviations (SD). For multiple comparisons two-way analyses of variance (ANOVA) with Bonferroni posttests were employed to determine the presence and extent of significant differences between groups.

4 RESULTS

4.1 Mouse model for Asm overexpression

4.1.1 Generation of the mouse model

To investigate the effects an increase in Asm activity has, a mouse model in which the Asm can be conditionally overexpressed (tAsm) was generated by the company genOway, France. As shown in Figure 3, the transgene was inserted at the *Hprt* locus on the X-chromosome in murine embryonic stem cells. The *Hprt* (hypoxanthine phosphoribosyltransferase) gene encodes an enzyme of the purine nucleotide salvage pathway. Therefore, using the *Hprt* "Quick Knock-in™" approach, correct insertion of targeting vectors can be screened for by selection of clones in which the previously partially deleted *Hprt* locus is repaired by homologous recombination. These repaired cells are able to survive in conditions that lack the substrates for *de novo* nucleotide synthesis (HAT medium).

The Asm transgene is expressed under the control of the ubiquitous CAG promoter (a fusion of the CMV immediate early enhancer and chicken β-actin promoter). A loxP flanked STOP cassette between the promoter and the transgene allows for conditional expression of the transgene by crossing the tAsm mice with mice expressing Cre recombinase. Depending on the promoter regulating Cre recombinase expression, time- or tissue-specific Asm expression can be attained.

4.1.2 Genotypes

To achieve a constitutive expression of the Asm in all tissues, tAsm mice were bred with E2a-Cre transgenic mice for this study. Under the control of the E2a promoter the Cre recombinase is expressed from the oocyte stage onwards.

Due to the X-chromosomal localization of the Asm transgene, there are three possible transgenic genotypes to consider when characterizing this mouse strain. Male mice carrying the transgene are hemizygous, as they only possess one X-chromosome. Female mice can either be hetero- or homozygous, carrying one or two altered X-chromosomes, respectively. Male wildtype littermates result from breeding of heterozygous females with hemizygous males. Female transgenic mice that were not interbred with Cre-mice were used as controls,

as they are carrying the transgene but do not express the protein, due to the STOP cassette remaining upstream of the transgenic cassette (see Figure 3).

Table 2 Genotypes
tAsm = Asm transgenic mice; fl = presence of loxP site, indicates insertion of the targeting vector in the X-chromosomal *Hprt* locus, 0 = refers to absence of *Hprt* locus (Y-chromosome), + = indicates a wildtype *Hprt* locus, E2a-Cre: presence (tg) or absence (wt) of a Cre recombinase under the control of the E2a promoter.

Sex	tAsm genotype	symbol	*Hprt* locus	E2a-Cre
male	**wildtype**	**♂ wt**	+/0	tg
	hemizygous	**tg/0**	fl/0	tg
female	**wildtype**	**♀ wt**	fl/fl	wt
	homozygous	**tg/tg**	fl/fl	tg
	heterozygous	**tg/+**	fl/+	tg

4.1.3 Physical development of the mice

To assess whether the overexpression of Asm impacts the development of mice with respect to growth, their body weight was monitored on a weekly basis throughout the age-span used for the investigations of this study. At an age of about 18-20 weeks the mice were fully grown and did not gain substantial amounts of weight anymore. As is true for wildtype mice, transgenic male mice had greater body mass than age-matched female mice. The development of those mice expressing the transgene, however, did not deviate significantly from that of gender-matched wildtype littermates (Figure 4). The outward appearance of the mice was normal.

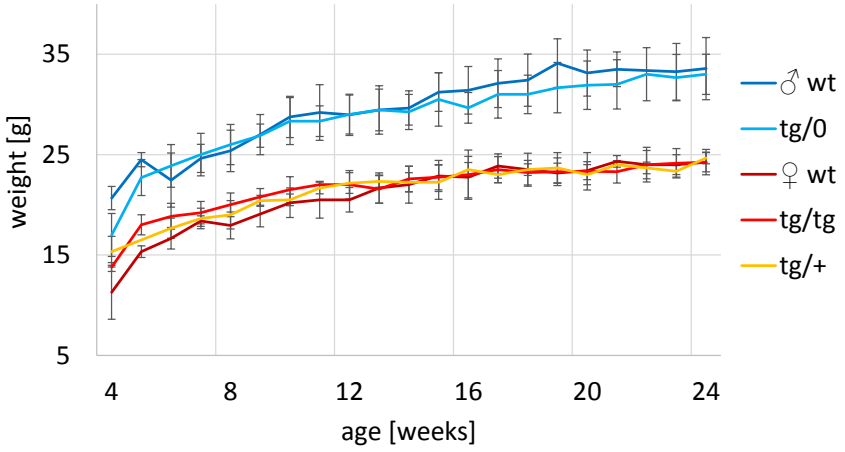

Figure 4 Weight curve
Depicted are the means ± SD of the weekly measurements of mouse body weight throughout the age-span used in the investigations; n ≥ 6

4.2 Sphingolipid metabolism of the lung

4.2.1 Enzyme activities

4.2.1.1 Acid sphingomyelinase activity

To assess the extent of the transgene's effect on Asm activity, an *in vitro* assay that measures the production of ceramide from a fluorescently labeled substrate (BODIPY™ FL C_{12}-sphingomyelin) was employed. In short, whole tissue lysates were assayed via incubation of 0,5 µg protein per sample with 100 pmol of the substrate at 37 °C for 1 hour under acidic conditions (pH 5,0). After the extraction of lipids and their separation via TLC, the relative fluorescence intensities of the reaction product and the unconsumed substrate were determined via a fluorescence laser scanner and subsequently used for the calculation of the Asm activity.

As displayed in Figure 5A, the Asm activity in the lungs of transgenic mice was about 10-fold higher than in their wildtype counterparts. For the most part there were no significant differences in the activities of male versus female mice. The exception to this was the Asm activity in lungs of 2 months old mice, which was lower in female transgenic than male transgenic mice. Across all transgenic mice there was a tendency for the activity to decrease as the mice age. However, these age-related differences reached a significant level solely in male transgenic mice when comparing the oldest set of mice to either of the other age groups.

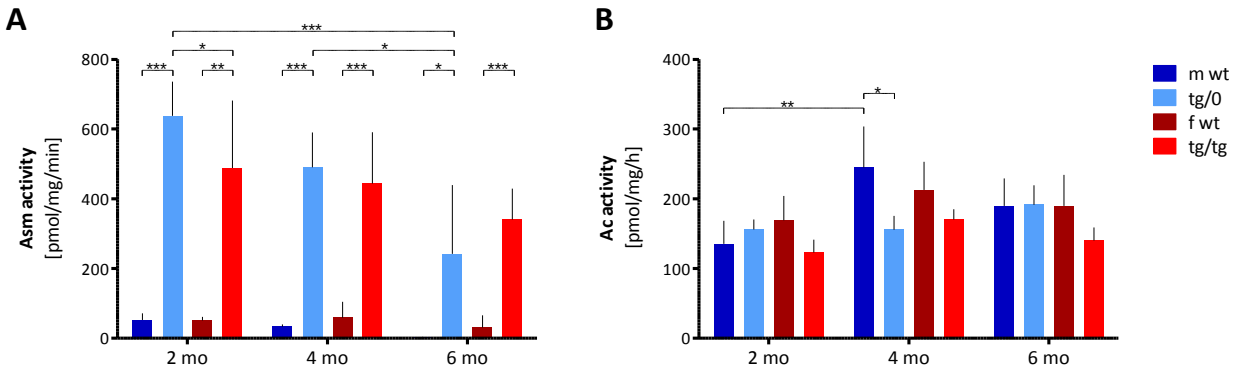

Figure 5 Asm and Ac activities
Enzyme activities for Asm (**A**) and Ac (**B**) of whole tissue lysates are displayed as means ± SD, n ≥ 3. Asterisks indicate levels of significance as calculated by two-way ANOVA with Bonferroni posttests * p < 0,05; ** p < 0,01; *** p < 0,001

4.2.1.2 Acid ceramidase activity

As the acid ceramidase (Ac) acts in a complex with the Asm (He *et al.* 2003), it seemed prudent to investigate whether the overexpression and increased activity of Asm occasions an elevation in Ac activity as well. The assay employed is essentially a recapitulation of the Asm activity assay, the two main differences being the substrate and the pH. The substrate used to assess Ac activity is a fluorescently labeled ceramide (NBD-C_{12}-ceramide). The pH for this assay is set to 4,5 to ensure optimal Ac activity, minimizing the reverse reaction of the enzyme (Okino *et al.* 2003). Also, as activity of the acid ceramidase is generally much lower than that of the acid sphingomyelinase (Teichgräber *et al.* 2008), this difference being not surprisingly exacerbated in mice containing an Asm transgene, a larger protein equivalent (i.e. 20 µg per sample) and an increased incubation period with the substrate (i.e. 3 h) was necessary to generate detectable levels of NBD-ceramide turnover.

The genotype of the mice and their associated Asm activities did not significantly alter the activity of the Ac (Figure 5B). There was a slight trend toward lower Ac activities especially in the female transgenic mice. This trend, however, only became significant in the male mice at 4 months of age. This lowered Ac activity in transgenic mice is in stark contrast to the elevated Asm activity. There was no age-related difference in Ac activity in male or female mice.

4.2.2 Lipid composition

Looking into the effect of expression of the transgene on the basal pulmonary lipid composition in tAsm mice, mass spectrometric analyses were conducted on powdered tissue of the left lung. Briefly, extracted lipids were spiked with internal standards and subjected to mass spectrometric analyses using HPLC quadrupole or triple quadrupole TOF mass spectrometers for sphingomyelin and ceramide or sphingosine quantification, respectively. The analyses were conducted in MS/MS mode using the respective fragmentations of precursor into product ions with their defined mass-to-charge ratios.

Figure 6 depicts total sphingomyelin and ceramide levels (A) as well as their respective species (B), differing in the length of the acyl chain, while panel C portrays the sphingosine content of the lungs. Tissues of all genotypes at the ages of 2, 4, and 6 months were analyzed.

For the most part sphingomyelin levels (left panels, Figure 6A+B) were not impacted by the overexpression of Asm. Surprisingly, an elevation in several sphingomyelin species was observed in six months old transgenic mice. As for younger mice at the age of 2 months,

sphingomyelin levels were quite uniform in all mice with the striking exception of female wildtype mice. The same was true for ceramide and sphingosine – 2 months old female wildtype mice displayed much higher levels of all lipid species per protein content of the tissue.

An increase in the overall ceramide levels (right panel, Figure 6A) upon Asm overexpression was only observed in 4 months old homozygous females. When looking in more detail, all ceramide species (right panel, Figure 6B) were elevated in these mice when compared to female wildtype mice. However, it only reached significant levels in ceramide with a monounsaturated acyl chain of 24 carbon atoms in length (C24:1). Analogous – though not significant – trends could be observed in male mice of the same age. In fully grown mice (6 months old) there was no increase in the total ceramide content of transgenic mice. Out of the various ceramide species, however, very long chain ceramides were more prone to accumulate in Asm-overexpressing mice. C24:1 ceramide showed significantly higher levels in male transgenic mice. The saturated as well as the monounsaturated C24 ceramide species were also meaningfully elevated in heterozygous females, yet not in their homozygous littermates. Overall the mature female homozygous mice showed surprisingly low levels of ceramide. While lungs of younger hemizygous and homozygous mice contained comparable levels of all species analyzed, homozygous mice at the age of 6 months had significantly lower levels of ceramide than their male counterparts.

Regarding sphingosine there were no effects on its levels due to Asm overexpression (Figure 6C). Differences observed in 2 months old mice were invariably due to the aforementioned unusually high levels of all lipids in the lungs of the female wildtype mice.

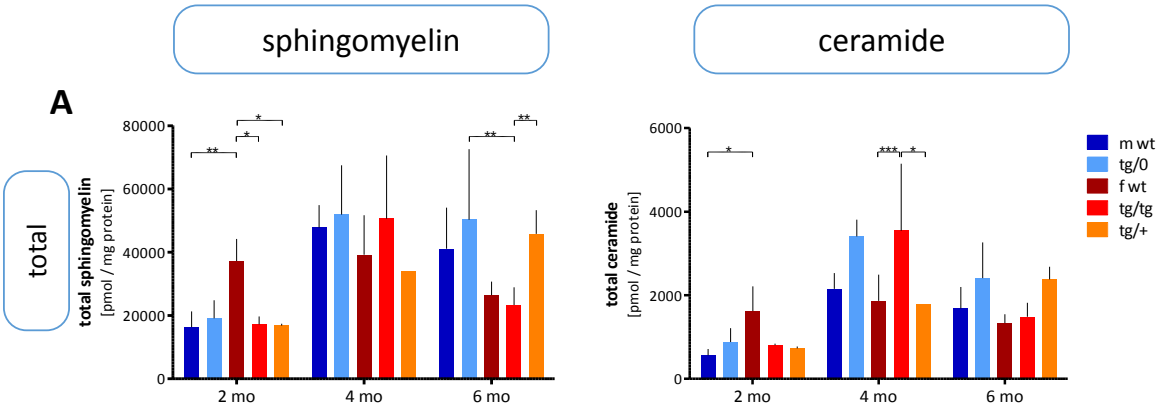

Figure 6 Lipid composition of murine lungs

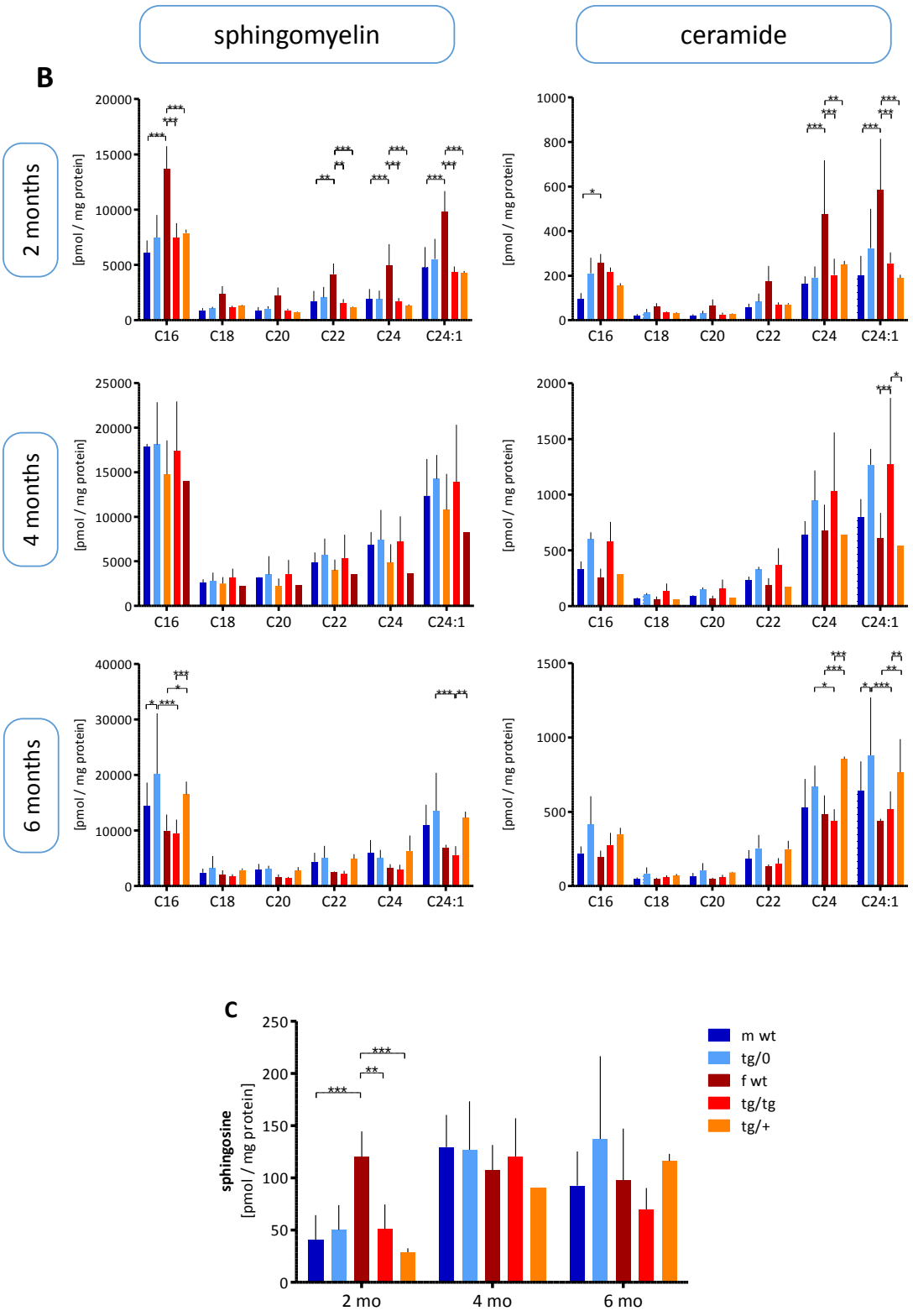

Figure 6 Lipid composition of murine lungs (continued)
The lipid content of murine lungs as determined by mass spectrometric analyses. Displayed are the total amounts of sphingomyelin and ceramide, respectively (**A**), the levels of sphingomyelin and ceramide species, distinguished by the length of their acyl chains (**B**), and the sphingosine content (**C**) as determined in lungs of mice aged 2, 4, and 6 months. The amounts of all lipids are normalized to the amount of protein present in the tissue samples, means ± SD are depicted, n = 1-7. Asterisks indicate levels of significance as calculated by two-way ANOVA with Bonferroni posttests * $p < 0,05$; ** $p < 0,01$; *** $p < 0,001$

4.2.3 Ceramide localization within lung tissue

To assess if and where ceramide produced by Asm accumulates in the tissue, lung sections were probed with a ceramide-specific antibody. To this end, paraffin-embedded superior and middle lobes of the right lung of transgenic and wildtype mice were cut into 6 µm thick sections. Following dewaxing and rehydration, ceramide was indirectly labeled with a Cy3 fluorophore, which was visualized using confocal microscopy. To test for unspecific binding of the Cy3-labeled secondary antibody to the tissue, stainings without addition of primary antibody were used as controls.

Endothelial cells showed very prominent staining for ceramide in all genotypes (Figure 7, arrow). In other cell types differential stainings in transgenic compared to wildtype lungs were observed. Especially the bronchial epithelial cells of transgenic mice showed much higher levels of ceramide than those of wildtype mice (Figure 7, arrowheads). This was true for both genders. Notably, ceramide accumulated predominantly in the apical regions of the epithelial cells of Asm-overexpressing mice.

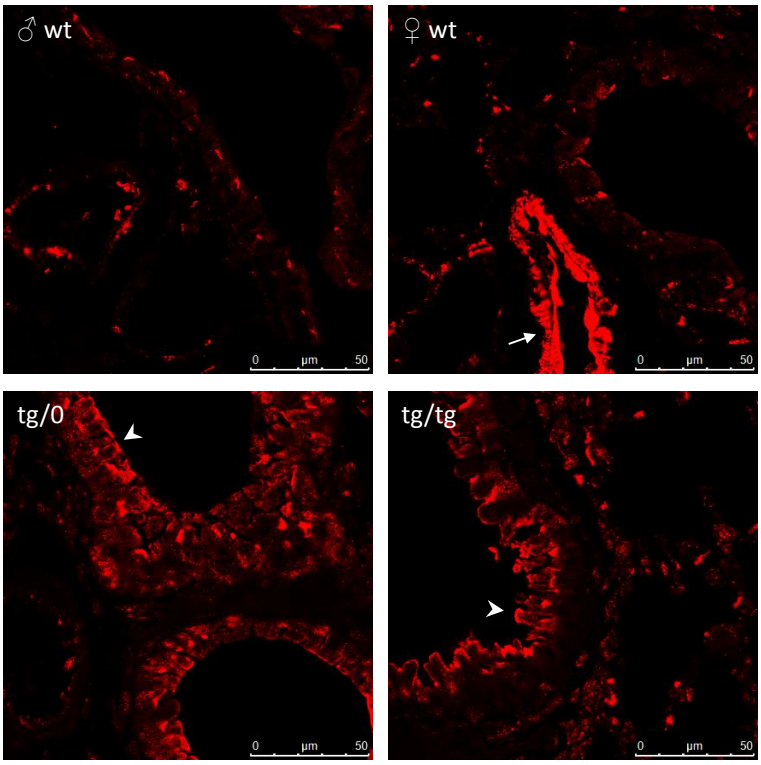

Figure 7 Bronchial ceramide accumulation
Specific detection of ceramide on lung sections visualized via Cy3 fluorescence. Exemplary pictures of lungs of wildtype and transgenic mice of both genders, aged 4 months. Ceramide stainings were predominant in endothelial cells (arrow) and the apical membrane of epithelial cells (arrowheads). Scale bars = 50 µm

4.3 Pulmonary morphology and histology

As changes in structure and composition of the lung tissue might result from the altered expression of the Asm and the concomitant changes in ceramide distribution, a screening for morphological aberrations was conducted.

Paraffin-embedded sections of the superior and middle lobes of the right lung were counterstained with hematoxylin and eosin (H&E) (Figure 8A). In some areas of the lung the alveolar septs of transgenic mice appeared thicker than in their wildtype littermates. To assess whether this is a local phenomenon or if alveolar septs of Asm-overexpressing mice are generally thicker, the thickness of septs was quantified in a randomized manner across whole tissue sections. Upon considering the measurements over large areas of the lung no difference in the thickness of the septs was found (Figure 8B).

As the activity of Asm has been implicated in the development of pulmonary fibrosis in cystic fibrosis mice (Ziobro *et al.* 2013), changes in the makeup of the connective tissue were assessed. To this end Masson's trichrome stain on paraffin-embedded sections as well as collagen quantification in fresh lung tissue were employed. Masson's stain is used for the study of connective tissue, staining collagen fibers (blue) in particular.

Figure 8C shows the staining of lung tissues of 4 months old mice. In both genders the overexpression of Asm did not lead to alterations of fiber content in the tissue. Comparable observations were made in 6 months old mice (data not shown).

Similarly, the quantification of lung collagen (Figure 8D) showed no differences among male mice. In female mice, however, differences between the genotypes could be observed. While at the age of 2 months there was a clear, if not significant, trend towards a decrease of the collagen content in transgenic compared to wildtype mice, the effect was significant but quite reversed in the 4 months old mice.

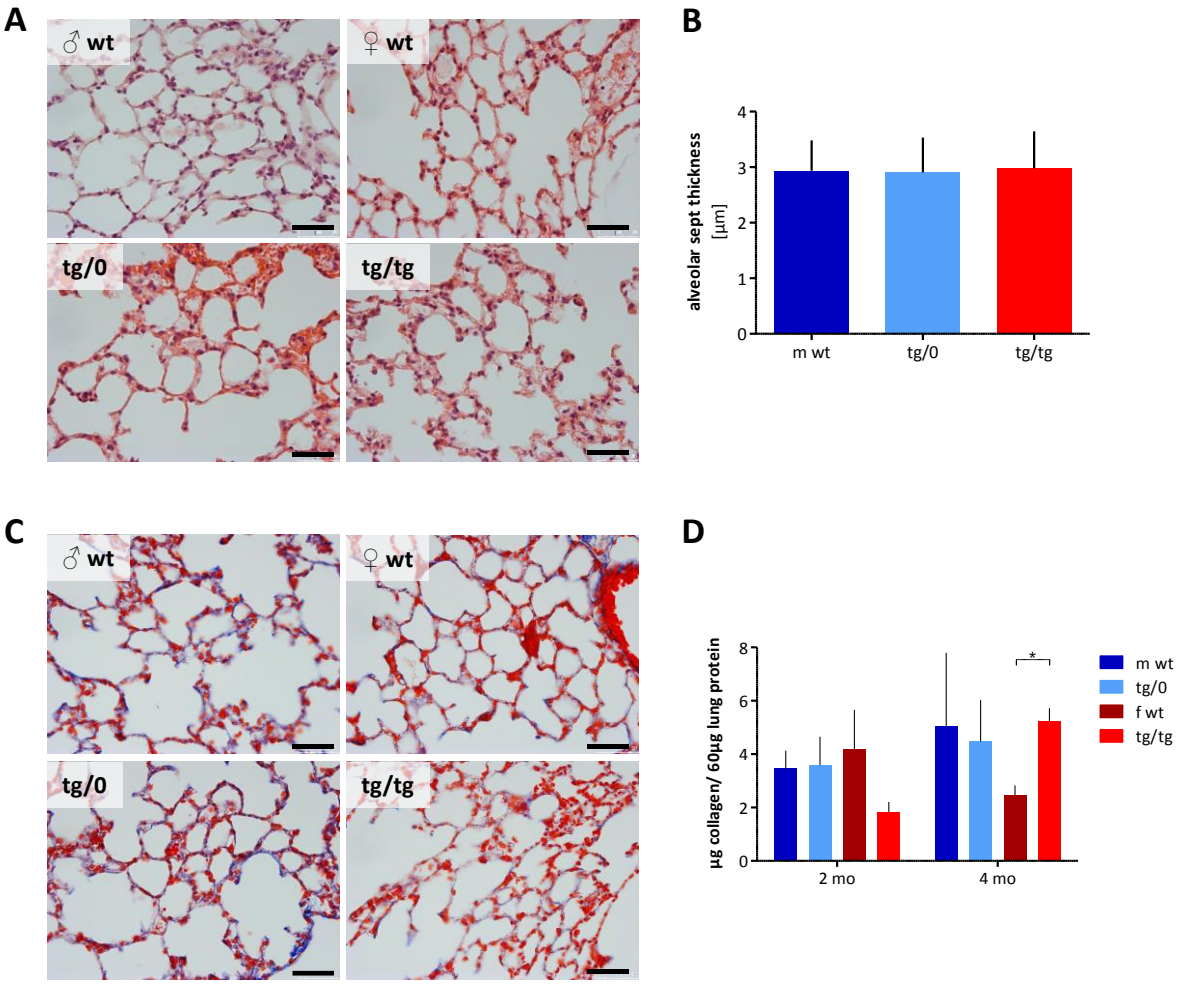

Figure 8 Pulmonary morphology and collagen content
A H&E stain and **C** Masson's trichrome stain of 6 µm lung sections of wildtype and transgenic mice of both genders, aged 4 months, scale bars = 50 µm **B** Quantification of alveolar sept thickness as measured on sections of mice, aged 2 months, a minimum of 400 septs per mouse were measured, depicted are means ± SD. **D** Quantification of soluble collagen in fresh lung tissues. The collagen content is normalized to the protein content of the tissue, depicted are means ± SD, n ≥ 3. The Asterisk indicates the level of significance as calculated by two-way ANOVA with Bonferroni posttests: * $p < 0,05$

4.4 Cellular infiltration and lung inflammation

While the fiber content of lungs was largely unaffected by Asm expression, the cellular infiltration was higher in transgenic compared to wildtype mice (Figure 8C). Neutrophils are commonly the first cells to infiltrate into inflamed or damaged tissues and are known to accumulate in lungs of CF mice (Laval 2016), which also show a ceramide distribution alike to that observed in our model (Figure 7; Grassmé *et al.* 2017).

To investigate whether the increased cellularity is caused by infiltrating neutrophils, tissue sections were probed with a neutrophil-specific antibody (Figure 9A). The quantification of neutrophils in lungs of 2 and 4 months old mice (Figure 9B) revealed no significant differences between wildtype and transgenic mice. Overall, however, lungs of male mice contained higher numbers of neutrophils than those of female mice.

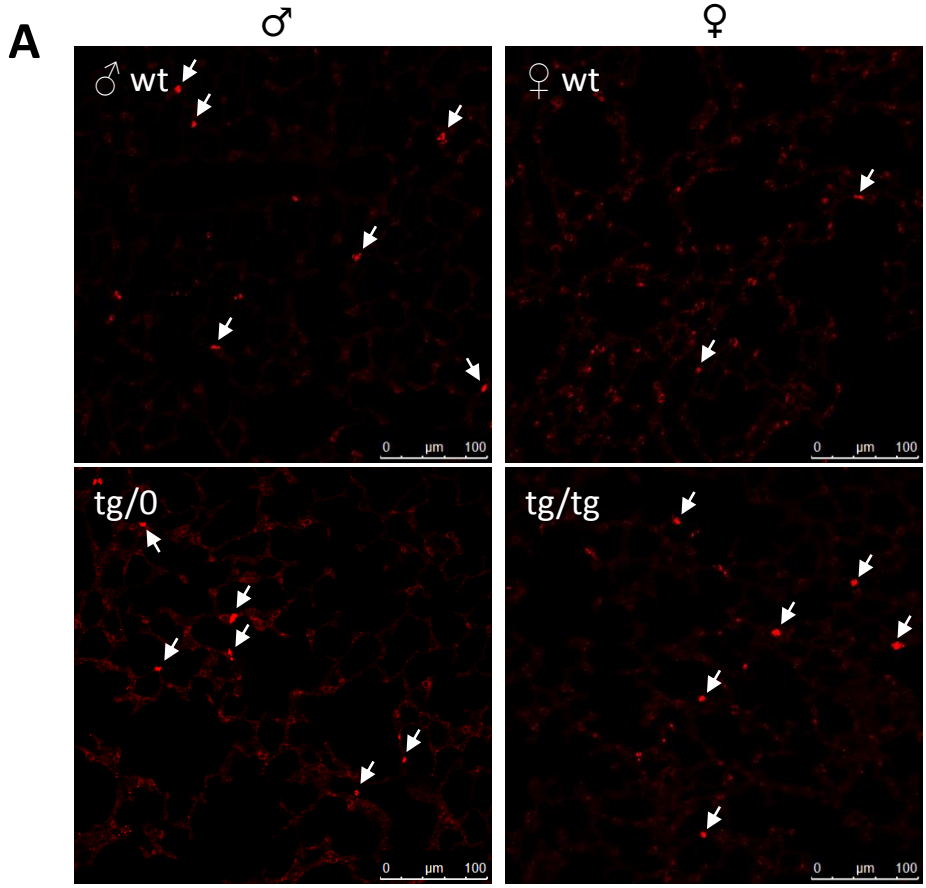

Figure 9 Infiltrating neutrophils in murine lungs
A Specific detection of Gr1-positive cells (arrows) on lung sections visualized via Cy3-fluorescence. Representative pictures of stainings in wildtype and transgenic mice of both genders, aged 4 months. Scale bars = 100 µm;

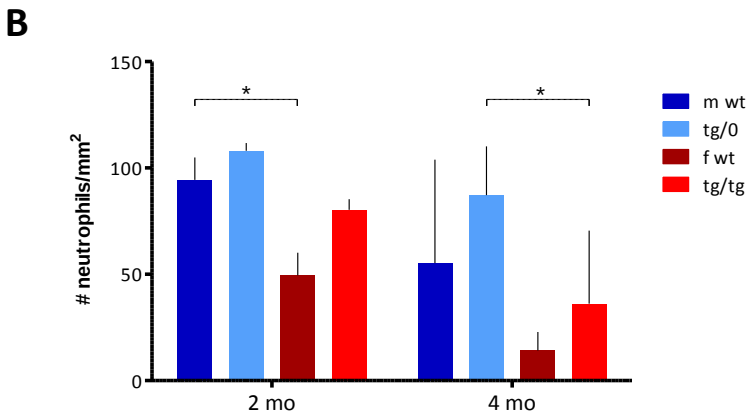

Figure 9 Infiltrating neutrophils in murine lungs (continued)
B Quantification of pulmonary Gr1-positive cells. Cells were counted in random areas of lung tissue sections of 2 and 4 months old wildtype and transgenic mice. Means ± SD are depicted, n= 3-4. Asterisks indicate levels of significance as calculated by two-way ANOVA with Bonferroni posttests * $p < 0,05$

Next, the effect of Asm overexpression on the inflammatory status of the mice - and their lungs specifically - was evaluated. Preliminary data on serum cytokine levels in older mice (7 months) on an array (Figure 10A+B), pointed towards differences regarding several cytokines. Among these were cytokines known to be involved in mobilization and differentiation of hematopoietic stem cells (G-CSF, GM-CSF, IL-3), chemoattractants for neutrophils and T-cells (KC/CXCL1, CXCL13), and cytokines that act as proinflammatory mediators (TNFα, TREM-1).

To gauge the inflammatory state of the lungs specifically, lung lysates were probed for IL-1β, IL-6, KC, TNFα and GM-CSF. These tissue cytokine levels were analyzed with the respective sandwich ELISA kits obtained from R&D Systems. In most instances (TNFα, GM-CSF, KC) however, the cytokine levels were below the detection limit of the kits. The levels of IL-6 in lungs of 4 months old mice as well as IL-1β in all three age groups (2, 4, and 6 months) are uniformly low across all genotypes (Figure 10C, D).

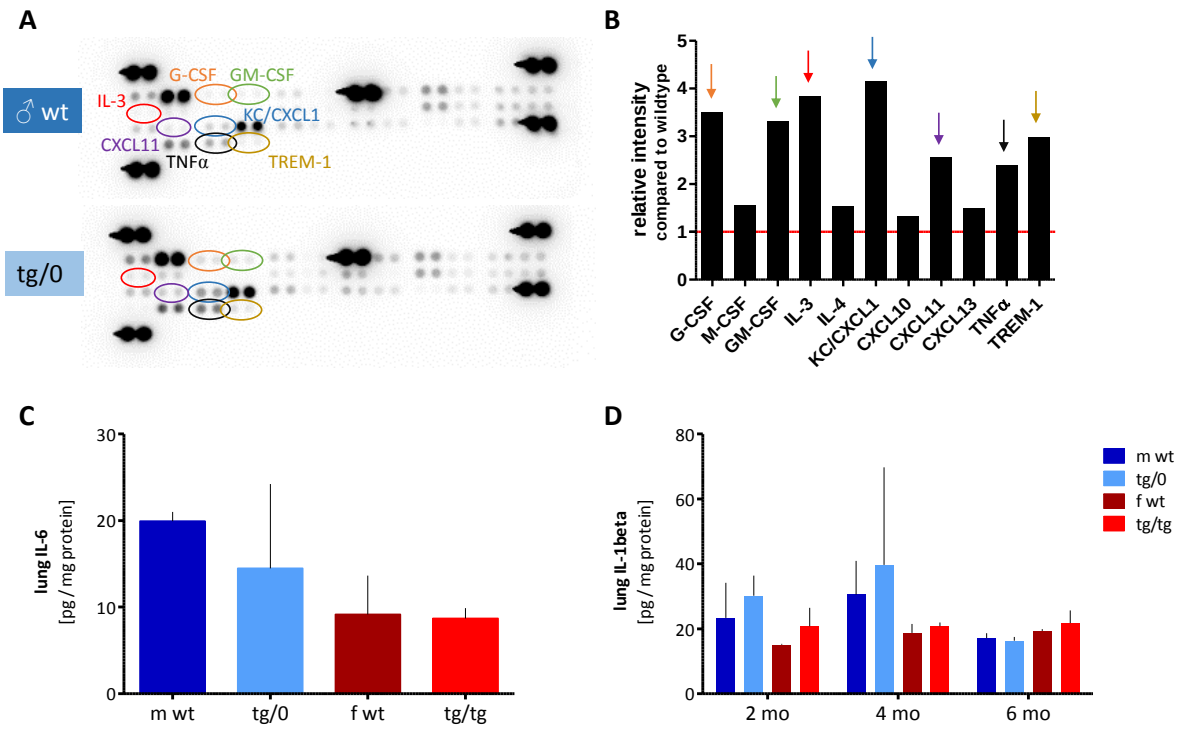

Figure 10 Serum and tissue cytokines
A Signal detection of serum cytokines of a male transgenic and a wildtype mouse aged 6 months on an array. Colored ellipses highlight array spots that showed differences between the two genotypes, correspondingly colored labels indicate the cytokine captured on the respective spots. **B** Depiction of the relative spot intensities of the transgenic mouse compared to wildtype, which is set to 1 (red line). Colored arrows point out cytokines labeled in **A**. Several tissue cytokines were detected in lung lysates. The graphs show levels of IL-6 in 4 months old mice (**C**), and IL-1β in mice of the indicated ages (**D**). Cytokine levels are given in pg cytokine per mg lung protein, columns represent means ± SD, n = 2

4.5 Autophagy

Sphingolipids in general have been shown to modulate autophagy. Ceramide in particular targets several regulators of autophagy to increase autophagic turnover (Jiang and Ogretmen 2014; Young *et al.* 2013). To investigate whether overexpression of Asm and the increase in ceramide affects autophagy levels in lung cells, several autophagy-associated proteins were probed for on blots of whole tissue lysates (Figure 11A). ULK1 initiates autophagosome formation. Its activity is differentially regulated by various phosphorylations. ULK1 phosphorylated at serine 555 results in induction of autophagy, while phosphorylation of serine 757 inhibits autophagosome formation. PP2A, pBeclin and p62 are directly or indirectly involved in the induction and progression of autophagy, whereas mTOR negatively regulates autophagy.

None of the investigated proteins' expression or phosphorylation/activation status was altered significantly in tAsm compared to wildtype mouse lungs.

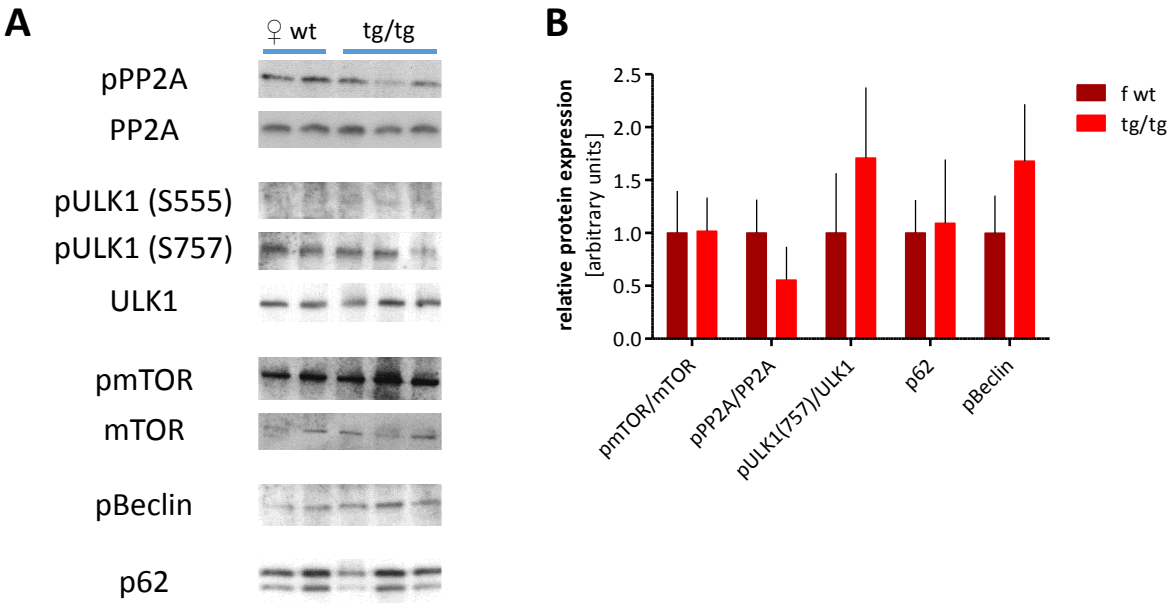

Figure 11 Autophagy-related proteins
A examples of western blots detecting various autophagy-related proteins in lung lysates of 4 months old female mice. **B** Relative expression of autophagy-related proteins. Fluorescence intensities were normalized to β-actin, wildtype protein levels were set to 1, bars depict means ± SD, n = 2-3

5 DISCUSSION

The acid sphingomyelinase is most clearly linked to human disease with respect to its deficiency in Niemann-Pick disease type A and B. However, the hyperactivity of ASM has been reported in connection with an increasing number of pathological states. Yet, models to specifically investigate its role in these settings were lacking. This study describes a mouse model of Asm overexpression which paves the way for such investigations. Here, it is demonstrated that the tAsm mouse model is suitable for investigations into the significance of the increased activity of the acid sphingomyelinase with a special focus on the lung phenotype. Further investigations are warranted with respect to other organs.

The transgenic mice used in this project were examined in an unchallenged state. The aim of the study was to characterize the mice under baseline conditions, without exposing them or any of their samples to an activating stimulus. A diverse set of stimuli have the ability to activate the Asm (Hannun and Obeid 2002). Also, the L-Asm and S-Asm can be stimulated by different triggers (Kornhuber *et al.* 2015). As such, they should be looked at separately, with the specific research question in mind.

Therefore, the data presented here only shows effects caused by the mere increased expression of the Asm as opposed to stimulus-induced activation. The question this aimed to answer was, whether these mice are a useful model for the study of diseases that have been associated with increased ASM activity. As such, this model constitutes a closure of the gap in available models. Previously available Asm mouse models were deficient in Asm expression and modelled Niemann-Pick disease (Horinouchi *et al.* 1995).

That being said, with respect to mere physical development no differences between the transgenic and wildtype mice were apparent (Figure 4). It should be noted, however, that the mice used in this study were comparatively young, being a maximum of 6 months old. This may be relevant, considering that a lot of the diseases associated with heightened ASM activity, usually manifest in humans at a later time in life (e.g. atherosclerosis, cardiovascular disease, Alzheimer's disease). However, it remains unclear how long (if at all) ASM activity has been raised before the onset of the disease. Especially for the study of the diseases mentioned above further studies on mice of older age are necessary.

Some differences in the generation of male and female mice should be noted. In the case of male mice, all mice are transgenic for the expression of Cre recombinase under the control of the E2A promoter. However, they differ in their expression of the Asm transgene for which they are either hemizygous or wildtype. In contrast, all the female mice possessed the Asm transgene – either homozygous or heterozygous – but they differed in their expression of Cre recombinase. Female mice designated as "wildtype" contain the Asm transgene, but have not been crossed with E2a-Cre mice, therefore the loxP flanked STOP cassette prevents the expression of the Asm transgene. The heterozygous animals are expected to present a mosaic expression pattern of the transgene. With organs or large cell clusters falling in line with either their homozygous or "wildtype" counterparts rather than somewhere in the middle. This is due to the random silencing of one of the two X chromosomes in each cell of the early embryo. This silencing is passed on to all the cells they give rise to subsequently (Boumil and Lee 2001).

Another factor contributing to the possibly differential expression of the transgene within one genotype is the modulation of transcription efficiencies due to methylation. It has been found in other transgenic mouse models using the CAG promoter, that promoter methylation can lead to different levels of expression of the transgene even among mice of the same litter (Zhou *et al.* 2014).

The EIIa promoter, controlling Cre expression, is active in oocytes and pre-implantation embryos. Thus, the loxP-flanked STOP cassette is excised in all cells of the mice (Dooley 1990).

The overexpression of Asm via the transgene clearly leads to an elevation of the sphingomyelinase activity per protein content of the lung (Figure 5A). This is consistent with previous published trends (Gulbins *et al.* 2013; Mühle *et al.* 2013). In the current study Asm activity in the lungs of transgenic mice was increased about 10-fold compared to wildtype mice. This matches the increase in Asm activity in the cerebrosphinal fluid (CSF) of tAsm compared to wildtype mice, while the reported difference in hippocampal samples was about 4-fold (Mühle *et al.* 2013; Gulbins *et al.* 2013). The assay employed in the present study was carried out with added zinc ions in the assay buffer, allowing for the detection of the activity of lysosomal and secretory Asm. Thus, the results from our experiments as well as those done on CSF samples, indicate that not only the intracellular Asm activity is increased due to the transgene, but also that of the secreted form of Asm. It is also clear that the extent of the increase of Asm activity varies between different cell types. Of note, the absolute values of

Asm activity are much lower in CSF samples, as there is much less protein present. The activity was also given relative to the volume of CSF rather than protein content. Also, in the study on CSF heterozygous mice were used for the analysis (Mühle 2013).

As the transgene leads to a higher expression of the Asm, the increased conversion of sphingomyelin in the *in vitro* assay is likely due to the increased amount of Asm present in the lungs of transgenic mice rather than an increased activity of the enzyme *in vivo*. However, this remains speculative, as the amount of Asm protein has not been determined in this study. Previous publications showed the increased amounts of Asm protein via immunofluorescence stainings of hippocampal sections of tAsm and wildtype mice (Gulbins *et al.* 2013). The Asm activity assay employs a substrate with a fluorescent group attached to the acyl chain of C12 sphingomyelin. Endogenous substrates cleaved by Asm usually contain acyl chains of 14 carbons and longer (Mullen *et al.* 2012). The assay, however, is well established and conveys a reliable impression of the enzyme's activity (Mühle and Kornhuber 2017).

It has not been investigated to what extend the transgene gives rise to secretory or lysosomal Asm. But since the endogenous *Smpd1* gene encodes both forms of Asm it is expected that the transgene does so as well. Especially increased amounts of secretory Asm would be expected to have systemic effects even under baseline conditions (Kornhuber *et al.* 2015). In a lot of settings it is unclear whether an activating stimulus triggers the release of secretory Asm or the translocation of lysosomal Asm to the plasma membrane. There is evidence that either is possible, depending on the trigger (Kornhuber *et al.* 2015). The constitutive release of large amounts of secretory Asm expressed from the transgene was hypothesized to override the need for an activating stimulus, since an increased amount of Asm would be present at the plasma membrane under baseline conditions. There is also evidence that Asm destined for the lysosome would be secreted, if the enzyme is expressed in such large amounts as to saturate the mannose 6-phosphate shuttle system to the lysosomes (Ioannou *et al.* 1992). The effects of increased amounts of Asm in the lysosome should be limited by the substrate availability. However, it is conceivable that the other enzymes involved in sphingolipid metabolism are outperformed by the increased amounts of Asm, which would be expected to lead to a lysosomal accumulation of ceramide. We specifically looked at Ac activity in the lungs of transgenic compared to wildtype mice, to check if there is a correlation. On the one hand this line of investigation was due reports of Asm and Ac forming a complex in the lysosome, working closely together (He *et al.* 2003). On the other hand, it has been recently

shown that the Asm transgenic mice show ectopic β1-integrin expression. This altered β1-integrin localization was subsequently linked to a down regulation of acid ceramidase (Grassmé *et al.* 2017). The data on acid ceramidase activity showed no significant difference in the lungs of tAsm compared to wildtype mice (Figure 5B). However, the activity was gauged *in vitro* via the conversion of a fluorescent substrate, this does not rule out a difference *in vivo*, considering that the overexpression of acid sphingomyelinase alters the lipid flux within the cell. Also, sphingolipid metabolism is well-known to shift and compensate for alterations (Hannun and Obeid 2011), so a look at effects on other enzymes involved in sphingolipid metabolism may reveal some interplay at work. Such effects can also be monitored with lipid profiles.

In this study the mass spectrometric analysis showed that for the most part ceramide and sphingosine levels are not altered in the transgenic mice (Figure 6). An increase in ceramide content in the lysosomes of Asm transgenic mice was expected. However, the mass spectrometry data only showed an increase in total ceramide levels in 4 months old female transgenic mice as well as for the most abundant ceramide species (C24:1) in 4 and 6 months old mice. Even though, there are trends towards increases in other ceramide species as well, especially in C16 ceramide. Much larger sample sizes will be need however, to see if these correlations are significant. For most data sets only samples from three mice were available. This may also account for the data in 6 months old female mice in which the heterozygous animals displayed higher ceramide and sphingomyelin levels than the transgenic animals. The lipid levels in the heterozygous females are comparable to those of the male transgenic mice, whereas the female homozygous transgenic mice are closer to the levels of wildtype mice. With respect to sphingomyelin, only in 6 months old male transgenic mice levels of C16 sphingomyelin, the most abundant species in lungs, were elevated compared to their wildtype counterparts. As it is, however, the data is not very robust. The standard deviation is quite high and can mask or over emphasize certain correlations. Especially the abnormally high lipid levels of the 2 months old female wildtype mice call into question how well these data can be interpreted, even though for this group specifically a larger data set was available (n=7). Furthermore, the influence of other enzymes involved in sphingolipid metabolism remains to be investigated. Enzymes involved in the turnover of ceramide, e.g. sphingomyelin synthase, ceramide kinase, or glycosylating enzymes, may show altered activities in tAsm mice due to compensatory mechanisms or simply altered substrate availability. Other studies across a

range of different models have found that the correlation of Asm activity and ceramide levels is not as clear cut, as may be expected. It is not uncommon to find that ceramide levels are unaltered or even reduced, even if the activity of acid sphingomyelinase is increased (Grammatikos *et al.* 2014; Drachman 2007; Lee *et al.* 2014).

In our mice C16 sphingomyelin is the most abundant sphingomyelin species, whereas C24 and C24:1 are the most abundant ceramide species. This was true regardless of the genotype. Diversity in the acyl chain length of sphingolipids is generated by ceramide synthases. Ceramide synthases (CerS) 2 and 5 have been found to be highly expressed in lungs (Xu *et al.* 2005; Petrache *et al.* 2013). CerS2 produces ceramide species C22 through C24, whereas CerS5 transfers acyl chains of 14 and 16 carbons in length to generate ceramide from sphingosine. Accordingly, it has been found that C24 and C16 ceramides and sphingomyelins are generally the most abundant species in lung tissue (Xu *et al.* 2005; Petrache *et al.* 2013). Furthermore, it has been shown that the ceramide species are in a delicate balance. Disrupting this homeostasis can increase the likelihood of inflammatory pulmonary diseases (Petrache *et al.* 2013).

For the most part the levels of S1P in this study were below the detection limit of the instrument, as S1P is not abundant in tissue but rather in the serum. Analyzing the serum of transgenic compared to wildtype mice might provide further insight into how the increased Asm expression affects downstream metabolites. S1P may prove of special interest, as it usually shows effects antagonizing those of ceramide (Newton *et al.* 2015).

A surprising finding was the trend in male mice of a decrease in the Asm activity with age. Studies with larger cohorts and a more extended time period should be conducted to verify this observation. If it should hold true, it should be investigated, if there is a similar relationship in humans and if this too is a sex-linked phenomenon. In fact, there already have been studies into alterations in sphingolipid metabolism in the course of a lifespan (Cutler 2001). In rats it has been shown, that the activity of the Asm increases with age in various tissues (Sacket *et al.* 2009). This observation is in line with reports on increased ASM activity in connection with various age-related diseases: Alzheimer's disease (Lee *et al.* 2014), chronic heart failure (Pan *et al.* 2014), diabetes mellitus type II (Górska *et al.* 2003), inflammatory renal disease (Kiprianos *et al.* 2012), non-alcoholic fatty liver (Grammatikos *et al.* 2014). Thus, the correlation between ASM activity and age in these cases is quite the reverse of what we

observed in this study. This may be due to ASM being a state rather than a trait marker for these diseases (Kornhuber *et al.* 2015). This means that the increase in ASM activity is secondary to the development of the diseases. In the case of our studies, the absence of activating triggers therefore does not entail an increase in Asm activity. It remains to be confirmed in further experiments, however, if the activity does decrease, if this trend continues for older mice and whether this is a sex-linked trait.

It is quite interesting to note that a lot of the diseases with Asm involvement show sex-dependent differences. Women are more prone to develop osteoporosis (Alswat 2017), Alzheimer's disease (Laws *et al.* 2018), clinical depression (Rainville *et al.* 2018), and autoimmune diseases in general (Voskuhl 2011). It is important to keep such differences in mind in future studies and account for them by doing investigations on male as well as female subjects. In mouse studies it often is not stated whether male or female mice were being used in an experiment. It is understood, though, that usually male mice are preferred, as they do not undergo cyclical hormonal changes. Any study should however first show that there are indeed no changes between the two sexes before proceeding to investigate only one of them. If differences become apparent it is vital to look at them more closely, to uncover by which mechanisms the responses in males and females differ, as this may affect treatment options and efficacies further down the line.

In this study there were hardly any differences observed between male and female mice. Apart from the decrease in Asm activity of aging male transgenic mice (Figure 5A), only the infiltration of neutrophils into the lung tissue showed sex-dependent differences (Figure 9). In the lungs of male mice at the age of 2 and 4 months there was a trend toward higher numbers of neutrophils than in female mice, irrespective of Asm genotype. While the neutrophil burden in the lungs of Asm transgenic mice is not as excessive as in CF mice, there are increased numbers of neutrophils in transgenic compared to wildtype mice (Figure 9). As our mice have not been challenged with a pathogen, our findings suggest that increased Asm expression and the thereby altered ceramide distribution is sufficient to induce neutrophil infiltration into the airways. Yet, this does not account for the differences between male and female mice. It has been shown that innate and adaptive immune responses are regulated in a sex-dependent manner (Jaillon *et al.* 2017). In general it has been found that females show enhanced innate immune responses, making them more resistant to infections while increasing the risk of autoimmune diseases. While estrogen activates various cells effector molecules of the

immune system, it also has restraining effects. The expression of IL-6 and Il-1β can be dampened by estrogen (Stein and Yang 1995; Hartwell *et al.* 2014). Estrogen has also been reported to modulate apoptosis, chemotaxis and recruitment of neutrophils (Molloy *et al.* 2003; Miyagi *et al.* 1992; Lasarte *et al.* 2016). In males on the other hand, the activation of neutrophils was shown to be increased during non-infectious inflammatory states (Deitch *et al.* 2006).

Cystic fibrosis (CF) lungs are characterized by large numbers of infiltrating neutrophils, whose inability to clear bronchial bacteria, leads to an exacerbated inflammatory response (Downey *et al.* 2009). Apart from the parallels in cellular infiltration, tAsm mice also mirror other pulmonary phenotypes of CF mice. Asm activity and ceramide accumulation has been associated with inflammatory signals with regard to multiple pathologies, including cystic fibrosis (Teichgräber *et al.* 2008). Notwithstanding the rather small differences in the ceramide content within the whole tissue lysates (Figure 6), the distribution of ceramide within the tissue and even within single cells did show marked differences between wildtype and transgenic mice (Figure 5). As has been previously published, in the apical membrane of lung epithelial cells of tAsm (and CF) mice, large ceramide platforms were observed (Grassmé *et al.* 2017, Figure 7). In wildtype mice endothelial cells showed high expression of ceramide, which is in accordance with previous reports (Marathe *et al.* 1998). The localization of ceramide at the apical surface of the bronchial epithelial cells suggests the activation and translocation of the Asm to that portion of the plasma membrane. This, however, usually happens in response to stress stimuli (Jenkins *et al.* 2009), which we did not induce in this setting. The constitutive release of secretory Asm may be responsible for this effect. Further investigations into the genesis of these ceramide platforms should be conducted.

The levels of serum as well as tissue cytokines are well worth looking into again. Due to limitations in sample availability, the amounts used in this work were well below the detection limit of the assay employed. Therefore, no definitive conclusions can be drawn from the data at hand as to the effects of overexpression of Asm on cytokine expression and release.

The similarities in ceramide abundance and localization between the tAsm and CF mice led us to investigate, whether other hallmarks of cystic fibrosis are apparent in the lungs of the tAsm mice. We could not find the same alterations in pulmonary morphology and collagen content found in CF mice, however (Ziobro *et al.* 2013, Figure 8). Thus, the increase in Asm expression

is not sufficient to influence changes in fiber content, which is more likely to have its causes elsewhere. It is important to note, though, that the measurements of alveolar sept thickness were only performed in one set of mice at the age of 2 months. Which does not rule out differences between wildtype and transgenic mice that arise later in life. The Masson's stain and the collagen measurements, however, were performed on lung tissue of 4 months old mice, which showed no significant differences at this time point either.

In my hands the pulmonary collagen quantification did not work very well and the reliability of the results is doubtful. The assay relies on the binding of a dye to collagen fibers. This dye however is prone to stick to other proteins as well. Even multiple washing steps and overnight digestion with pepsin did not yield the called for transparent sample pellet. While this assay seems to work very well with cultured cells, usage of unperfused tissue poses major challenges. For further studies it is advisable to adjust this method according to recommendations on improved accuracy (Lareu *et al.* 2010; Coentro *et al.* 2017).

Recently, an involvement of Asm and ceramide in the induction of apoptosis has been demonstrated for hippocampal tissue using - among others - tAsm mice (Gulbins *et al.* 2018). In hippocampi of Asm transgenic mice were shown to express lower amounts or show less activation of autophagy-related proteins than wildtype mice. This was associated with symptoms of depression in the tAsm mice as reported previously (Gulbins *et al.* 2018; Gulbins *et al.* 2013). Treatment with functional Asm inhibitors or an inhibitor of sphingomyelin synthase normalized the expression or activation of autophagy-related proteins and relieved depression symptoms (Gulbins *et al.* 2018). In contrast to that study, here no differences between wildtype and transgenic mice were apparent within the lung tissue samples (Figure 11). However, sample size was very small and the quality of the data is not very good. While differences in the autophagy induction at the tissue level are also conceivable, there have been studies showing that inhibition of acid sphingomyelinase triggers autophagy in pulmonary cells and tissues (Justice 2018). In that study, however, the effect on autophagy was correlated with altered sphingosine levels with subsequent alterations in S1P being implicated (Justice 2018). Dihydroceramides have also been shown to impact autophagy regulation in lungs (Mizumura *et al.* 2018). The mechanisms in autophagy regulation are very complex and multi-layered and are in need of further investigations with regards to tAsm lungs.

Overall, it can be said that tAsm mice need to be further characterized not only with regards to their pulmonary phenotype but also with respect to other organs. As the effects of Asm are connected to a wide range of issues, these mice can be of importance for studies into various diseases. The mice are not affected by a severe phenotype at baseline, so they provide a good basis for monitoring the effects of stressors, infections or additional genetic alterations. The loxP flanked STOP cassette upstream of the transgene also allows for time or tissue specific expression via Cre recombinase. Studies using these mice that have already been published also show their value as controls with respect to studies on Asm deficiency or inhibition (Gulbins *et al.* 2013; Grassmé *et al.* 2017; Gulbins *et al.* 2018). They may also be of further use in investigations into new drugs regulating Asm activity.

6 REFERENCES

Abdel Shakor A. B., Kwiatkowska K., Sobota A. (2004) Cell surface ceramide generation precedes and controls FcgammaRII clustering and phosphorylation in rafts. *J. Biol. Chem.* **279**, 36778–87.

Ali M., Fritsch J., Zigdon H., Pewzner-Jung Y., Schütze S., Futerman A. H. (2013) Altering the sphingolipid acyl chain composition prevents LPS/GLN-mediated hepatic failure in mice by disrupting TNFR1 internalization. *Cell Death Dis.* **4**, e929.

Alswat K. A. (2017) Gender Disparities in Osteoporosis. *J. Clin. Med. Res.* **9**, 382–387.

Avota E., Gulbins E., Schneider-Schaulies S. (2011) DC-SIGN mediated sphingomyelinase-activation and ceramide generation is essential for enhancement of viral uptake in dendritic cells. *PLoS Pathog.* **7**.

Baker D. A., Barth J., Chang R., Obeid L. M., Gilkeson G. S. (2010) Genetic sphingosine kinase 1 deficiency significantly decreases synovial inflammation and joint erosions in murine TNF-alpha-induced arthritis. *J. Immunol.* **185**, 2570–9.

Bauer J., Liebisch G., Hofmann C., Huy C., Schmitz G., Obermeier F., Bock J. (2009) Lipid alterations in experimental murine colitis: Role of ceramide and imipramine for matrix metalloproteinase-1 expression. *PLoS One* **4**, 1–8.

Becker K. A., Riethmüller J., Seitz A. P., Gardner A., Boudreau R., Kamler M., Kleuser B., et al. (2018) Sphingolipids as targets for inhalation treatment of cystic fibrosis. *Adv. Drug Deliv. Rev.* **133**, 66–75.

Becker K. A., Tümmler B., Gulbins E., Grassmé H. (2010) Accumulation of ceramide in the trachea and intestine of cystic fibrosis mice causes inflammation and cell death. *Biochem. Biophys. Res. Commun.* **403**, 368–374.

Beckmann N. (2017) Identification of novel clinical applications for acid sphingomyelinase inhibitors.

Beckmann N., Kadow S., Schumacher F., Göthert J. R., Kesper S., Draeger A., Schulz-Schaeffer W. J., et al. (2018) Pathological manifestations of Farber disease in a new mouse model. *Biol. Chem.* **399**, 1183–1202.

Beckmann N., Sharma D., Gulbins E., Becker K. A., Edelmann B. (2014) Inhibition of acid sphingomyelinase by tricyclic antidepressants and analogons. *Front. Physiol.* **5 AUG**, 1–14.

BERTHET J., SUTHERLAND E. W., RALL T. W. (1957) The assay of glucagon and epinephrine with use of liver homogenates. *J. Biol. Chem.* **229**, 351–61.

Bismarck P. Von, Wistädt C. F. G., Klemm K., Winoto-Morbach S., Uhlig U., Schütze S., Adam D., Lachmann B., Uhlig S., Krause M. F. (2008) Improved pulmonary function by acid sphingomyelinase inhibition in a newborn piglet lavage model. *Am. J. Respir. Crit. Care Med.* **177**, 1233–1241.

Borowitz D. (2015) CFTR, bicarbonate, and the pathophysiology of cystic fibrosis. *Pediatr. Pulmonol.* **50 Suppl 40**, S24–S30.

Boumil R. M., Lee J. T. (2001) Forty years of decoding the silence in X-chromosome inactivation. *Hum. Mol. Genet.* **10**, 2225–32.

Brady R. O., Kanfer J. N., Mock M. B., Fredrickson D. S. (1966) The metabolism of sphingomyelin. II. Evidence of an enzymatic deficiency in Niemann-Pick diseae. *Proc. Natl. Acad. Sci. U. S. A.* **55**, 366–9.

Brown D. A. (2006) Lipid Rafts, Detergent-Resistant Membranes, and Raft Targeting Signals. *Physiology* **21**, 430–439.

Camell C. D., Nguyen K. Y., Jurczak M. J., Christian B. E., Shulman G. I., Shadel G. S., Dixit V. D. (2015) Macrophage-specific de Novo Synthesis of Ceramide Is Dispensable for Inflammasome-driven Inflammation and Insulin Resistance in Obesity. *J. Biol. Chem.* **290**, 29402–13.

Charruyer A., Grazide S., Bezombes C., Müller S., Laurent G., Jaffrézou J. P. (2005) UV-C light induces raft-associated acid sphingomyelinase and JNK activation and translocation independently on a nuclear signal. *J. Biol. Chem.* **280**, 19196–19204.

Coentro J. Q., Capella-Monsonís H., Graceffa V., Wu Z., Mullen A. M., Raghunath M., Zeugolis D. I. (2017) Collagen Quantification in Tissue Specimens, pp. 341–350.

Cremesti A., Paris F., Grassmé H., Holler N., Tschopp J., Fuks Z., Gulbins E., Kolesnick R. (2001) Ceramide Enables Fas to Cap and Kill. *J. Biol. Chem.* **276**, 23954–23961.

Cutler R. (2001) Sphingomyelin and ceramide as regulators of development and lifespan. *Mech. Ageing Dev.* **122**, 895–908.

Cyster J. G., Schwab S. R. (2012) Sphingosine-1-phosphate and lymphocyte egress from lymphoid organs. *Annu. Rev. Immunol.* **30**, 69–94.

Davis P. B. (2006) Cystic Fibrosis Since 1938. *Am. J. Respir. Crit. Care Med.* **173**, 475–482.

Deitch E. A., Ananthakrishnan P., Cohen D. B., Xu D. Z., Feketeova E., Hauser C. J. (2006) Neutrophil activation is modulated by sex hormones after trauma-hemorrhagic shock and burn injuries. *Am. J. Physiol. Circ. Physiol.* **291**, H1456–H1465.

Devlin C. M., Leventhal A. R., Kuriakose G., Schuchman E. H., Williams K. J., Tabas I. (2008) Acid Sphingomyelinase Promotes Lipoprotein Retention Within Early Atheromata and Accelerates Lesion Progression. *Arterioscler. Thromb. Vasc. Biol.* **28**, 1723–1730.

Di A., Kawamura T., Gao X.-P., Tang H., Berdyshev E., Vogel S. M., Zhao Y.-Y., et al. (2010) A Novel Function of Sphingosine Kinase 1 Suppression of JNK Activity in Preventing Inflammation and Injury. *J. Biol. Chem.* **285**, 15848–15857.

Dobrowsky R. T., Hannun Y. A. (1992) Ceramide stimulates a cytosolic protein phosphatase. *J. Biol. Chem.* **267**, 5048–5051.

Dobrowsky R. T., Kamibayashi C., Mumby M. C., Hannun Y. A. (1993) Ceramide activates heterotrimeric protein phosphatase 2A. *J. Biol. Chem.* **268**, 15523–30.

Dodge J. A., Lewis P. A., Stanton M., Wilsher J. (2007) Cystic fibrosis mortality and survival in the UK: 1947-2003. *Eur. Respir. J.* **29**, 522–526.

Downey D. G., Bell S. C., Elborn J. S. (2009) Neutrophils in cystic fibrosis. *Thorax* **64**, 81–8.

Drachman D. A. (2007) Rethinking Alzheimer's disease: the role of age-related changes. *Curr. Neurol. Neurosci. Rep.* **7**, 265–8.

Dumitru C. A., Gulbins E. (2006) TRAIL activates acid sphingomyelinase via a redox mechanism and releases ceramide to trigger apoptosis. *Oncogene* **25**, 5612–5625.

Edelmann B., Bertsch U., Tchikov V., Winoto-Morbach S., Perrotta C., Jakob M., Adam-Klages S., Kabelitz D., Schütze S. (2011) Caspase-8 and caspase-7 sequentially mediate proteolytic activation of acid sphingomyelinase in TNF-R1 receptosomes. *EMBO J.* **30**, 379–394.

Filippov V., Song M. A., Zhang K., Vinters H. V., Tung S., Kirsch W. M., Yang J., Duerksen-Hughes P. J. (2012) Increased ceramide in brains with alzheimer's and other neurodegenerative diseases. *J. Alzheimer's Dis.* **29**, 537–547.

Fujiwara N., Usui T., Ohama T., Sato K. (2016) Regulation of Beclin 1 Protein Phosphorylation and Autophagy by Protein Phosphatase 2A (PP2A) and Death-associated Protein Kinase 3 (DAPK3). *J. Biol. Chem.* **291**, 10858–10866.

Futerman A. H., Hannun Y. A. (2004) The complex life of simple sphingolipids. *EMBO Rep.* **5**, 777–82.

Gable K., Gupta S. D., Han G., Niranjanakumari S., Harmon J. M., Dunn T. M. (2010) A disease-causing mutation in the active site of serine palmitoyltransferase causes catalytic promiscuity. *J. Biol. Chem.* **285**, 22846–22852.

Gagliostro V., Casas J., Caretti A., Abad J. L., Tagliavacca L., Ghidoni R., Fabrias G., Signorelli P. (2012) Dihydroceramide delays cell cycle G1/S transition via activation of ER stress and induction of autophagy. *Int. J. Biochem. Cell Biol.* **44**, 2135–2143.

Galadari S., Rahman A., Pallichankandy S., Galadari A., Thayyullathil F. (2013) Role of ceramide in diabetes mellitus: Evidence and mechanisms. *Lipids Health Dis.* **12**, 1.

Garcia D., Shaw R. J. (2017) AMPK: Mechanisms of Cellular Energy Sensing and Restoration of Metabolic Balance. *Mol. Cell* **66**, 789–800.

Gomes L. C., Dikic I. (2014) Autophagy in Antimicrobial Immunity. *Mol. Cell* **54**, 224–233.

Gorelik A., Illes K., Heinz L. X., Superti-Furga G., Nagar B. (2016) Crystal structure of mammalian acid sphingomyelinase. *Nat. Commun.* **7**, 1–9.

Górska M., Barańczuk E., Dobrzyń A. (2003) Secretory Zn2+-dependent sphingomyelinase activity in the serum of patients with type 2 diabetes is elevated. *Horm. Metab. Res.* **35**, 506–507.

Grammatikos G., Mühle C., Ferreiros N., Schroeter S., Bogdanou D., Schwalm S., Hintereder G., et al. (2014) Serum acid sphingomyelinase is upregulated in chronic hepatitis C infection and non alcoholic fatty liver disease. *Biochim. Biophys. Acta - Mol. Cell Biol. Lipids* **1841**, 1012–1020.

Grassmé H., Carpinteiro A., Edwards M. J., Gulbins E., Becker K. A. (2014) Regulation of the Inflammasome by Ceramide in Cystic Fibrosis Lungs. *Cell. Physiol. Biochem.* **34**, 45–55.

Grassmé H., Cremesti A., Kolesnick R., Gulbins E. (2003) Ceramide-mediated clustering is required for CD95-DISC formation. *Oncogene* **22**, 5457–5470.

Grassmé H., Henry B., Ziobro R., Becker K. A., Riethmüller J., Gardner A., Seitz A. P., et al. (2017) β1-Integrin Accumulates in Cystic Fibrosis Luminal Airway Epithelial Membranes and Decreases Sphingosine, Promoting Bacterial Infections. *Cell Host Microbe* **21**, 707-718.e8.

Grassmé H., Riehle A., Wilker B., Gulbins E. (2005) Rhinoviruses infect human epithelial cells via ceramide-enriched membrane platforms. *J. Biol. Chem.* **280**, 26256–26262.

Grin'kina N. M., Karnabi E. E., Damania D., Wadgaonkar S., Muslimov I. A., Wadgaonkar R. (2012) Sphingosine kinase 1 deficiency exacerbates LPS-induced neuroinflammation. *PLoS One* **7**, e36475.

Grösch S., Alessenko A. V., Albi E. (2018) The Many Facets of Sphingolipids in the Specific Phases of Acute Inflammatory Response. *Mediators Inflamm.* **2018**, 1–12.

Guenther G. G., Peralta E. R., Rosales K. R., Wong S. Y., Siskind L. J., Edinger A. L. (2008) Ceramide starves cells to death by downregulating nutrient transporter proteins. *Proc. Natl. Acad. Sci. U. S. A.* **105**, 17402–7.

Gulbins A., Schumacher F., Becker K. A., Wilker B., Soddemann M., Boldrin F., Müller C. P., et al. (2018) Antidepressants act by inducing autophagy controlled by sphingomyelin–ceramide. *Mol. Psychiatry* **23**, 2324–2346.

Gulbins E., Palmada M., Reichel M., Lüth A., Böhmer C., Amato D., Müller C. P., et al. (2013) Acid sphingomyelinase–ceramide system mediates effects of antidepressant drugs. *Nat. Med.* **19**, 934–938.

Gulbins E., Szabo I., Baltzer K., Lang F. (1997) Ceramide-induced inhibition of T lymphocyte voltage-gated potassium channel is mediated by tyrosine kinases. *Proc. Natl. Acad. Sci.* **94**, 7661–7666.

Haass N. K., Nassif N., McGowan E. M. (2015) Switching the sphingolipid rheostat in the treatment of diabetes and cancer comorbidity from a problem to an advantage. *Biomed Res. Int.* **2015**.

Hankins J. L., Fox T. E., Barth B. M., Unrath K. A., Kester M. (2011) Exogenous ceramide-1-phosphate reduces lipopolysaccharide (LPS)-mediated cytokine expression. *J. Biol. Chem.* **286**, 44357–66.

Hannun Y. A., Obeid L. M. (2002) The Ceramide-centric universe of lipid-mediated cell regulation: stress encounters of the lipid kind. *J. Biol. Chem.* **277**, 25847–50.

Hannun Y. A., Obeid L. M. (2011) Many ceramides. *J. Biol. Chem.* **286**, 27855–62.

Hartwell H. J., Petrosky K. Y., Fox J. G., Horseman N. D., Rogers A. B. (2014) Prolactin prevents hepatocellular carcinoma by restricting innate immune activation of c-Myc in mice. *Proc. Natl. Acad. Sci. U. S. A.* **111**, 11455–60.

Harvald E. B., Olsen A. S. B., Færgeman N. J. (2015) Autophagy in the light of sphingolipid metabolism. *Apoptosis* **20**, 658–70.

Hauck C. R., Grassmé H., Bock J., Jendrossek V., Ferlinz K., Meyer T. F., Gulbins E. (2000) Acid sphingomyelinase is involved in CEACAM receptor-mediated phagocytosis of Neisseria gonorrhoeae. *FEBS Lett.* **478**, 260–266.

He X., Huang Y., Li B., Gong C.-X., Schuchman E. H. (2010) Deregulation of sphingolipid metabolism in Alzheimer's disease. *Neurobiol. Aging* **31**, 398–408.

He X., Okino N., Dhami R., Dagan A., Gatt S., Schulze H., Sandhoff K., Schuchman E. H. (2003) Purification and characterization of recombinant, human acid ceramidase. Catalytic reactions and interactions with acid sphingomyelinase. *J. Biol. Chem.* **278**, 32978–86.

Heinrich M., Wickel M., Schneider-Brachert W., Sandberg C., Gahr J., Schwandner R., Weber T., Brunner J., Krönke M., Schütze S. (1999) Cathepsin D targeted by acid sphingomyelinase-derived ceramide. *EMBO J.* **18**, 5252–5263.

Herschkovitz A., Liu Y. F., Ilan E., Ronen D., Boura-Halfon S., Zick Y. (2007) Common inhibitory serine sites phosphorylated by IRS-1 kinases, triggered by insulin and inducers of insulin resistance. *J. Biol. Chem.* **282**, 18018–18027.

Horinouchi K., Erlich S., Perl D. P., Ferlinz K., Bisgaier C. L., Sandhoff K., Desnick R. J., Stewart C. L., Schuchman E. H. (1995) Acid sphingomyelinase deficient mice: a model of types A and B Niemann–Pick disease. *Nat. Genet.* **10**, 288–293.

Horn A. S. (1980) The mode of action of tricyclic antidepressants: a brief review of recent progress. *Postgrad. Med. J.* **56 Suppl 1**, 9–12.

Hurwitz R., Ferlinz K., Sandhoff K. (1994) The tricyclic antidepressant desipramine causes proteolytic degradation of lysosomal sphingomyelinase in human fibroblasts. *Biol. Chem. Hoppe. Seyler.* **375**, 447–50.

Huwiler A., Fabbro D., Pfeilschifter J. (1998) Selective Ceramide Binding to Protein Kinase C-α and -δ Isoenzymes in Renal Mesangial Cells †. *Biochemistry* **37**, 14556–14562.

Huwiler A., Johansen B., Skarstad A., Pfeilschifter J., Pharmakologie Z. Der (2000) Ceramide binds to the CaLB domain of cytosolic phospholipase A 2 and facilitates its membrane docking and arachidonic acid release.

Ioannou Y. A., Bishop D. F., Desnick R. J. (1992) Overexpression of human alpha-galactosidase A results in its intracellular aggregation, crystallization in lysosomes, and selective secretion. *J. Cell Biol.* **119**, 1137–1150.

Iwabuchi K. (2018) Gangliosides in the Immune System: Role of Glycosphingolipids and Glycosphingolipid-Enriched Lipid Rafts in Immunological Functions, in *Methods Mol. Biol.*, Vol. 1804, pp. 83–95.

Jaillon S., Berthenet K., Garlanda C. (2017) Sexual Dimorphism in Innate Immunity. *Clin. Rev. Allergy Immunol.*

Jenkins R. W., Canals D., Hannun Y. A. (2009) Roles and regulation of secretory and lysosomal acid sphingomyelinase. *Cell. Signal.* **21**, 836–46.

Jenkins R. W., Idkowiak-Baldys J., Simbari F., Canals D., Roddy P., Riner C. D., Clarke C. J., Hannun Y. A. (2011) A novel mechanism of lysosomal acid sphingomyelinase maturation: Requirement for carboxyl-terminal proteolytic processing. *J. Biol. Chem.* **286**, 3777–3788.

Jiang W., Ogretmen B. (2014) Autophagy paradox and ceramide. *Biochim. Biophys. Acta* **1841**, 783–92.

Kaibuchis K., Takai Y., Nishizuka Y. (1981) Cooperative Roles. **256**, 7146–7149.

Kanfer J. N., Young O. M., Shapiro D., Brady R. (1966) The Metabolism of Sphingomyelin. **241**.

Kasumov T., Li L., Li M., Gulshan K., Kirwan J. P., Liu X., Previs S., Willard B., Smith J. D., McCullough A. (2015) Ceramide as a mediator of non-alcoholic fatty liver disease and associated atherosclerosis. *PLoS One* **10**, 1–26.

Kim J., Kundu M., Viollet B., Guan K.-L. (2011) AMPK and mTOR regulate autophagy through direct phosphorylation of Ulk1. *Nat. Cell Biol.* **13**, 132–141.

Kinnunen P. K. J., Holopainen J. M. (2002) Sphingomyelinase Activity of LDL : A Link between Atherosclerosis , Ceramide , and Apoptosis ? **12**, 37–42.

Kiprianos A. P., Morgan M. D., Little M. A., Harper L., Bacon P. A., Young S. P. (2012) Elevated active secretory sphingomyelinase in antineutrophil cytoplasmic antibody-associated primary systemic vasculitis. *Ann. Rheum. Dis.* **71**, 1100–1102.

Kobayashi T., Stang E., Fang K. S., Moerloose P. de, Parton R. G., Gruenberg J. (1998) A lipid associated with the antiphospholipid syndrome regulates endosome structure and function. *Nature* **392**, 193–197.

Kolesnick R. N., Goni F. M., Alonso A. (2000) Compartmentalization of ceramide signaling: physical foundations and biological effects. *J. Cell. Physiol.* **184**, 285–300.

Kolter T., Sandhoff K. (2006) Sphingolipid metabolism diseases. *Biochim. Biophys. Acta - Biomembr.* **1758**, 2057–2079.

Kölzer M., Werth N., Sandhoff K. (2004) Interactions of acid sphingomyelinase and lipid bilayers in the presence of the tricyclic antidepressant desipramine. *FEBS Lett.* **559**, 96–98.

Kornhuber J., Medlin A., Bleich S., Jendrossek V. (2005) High activity of acid sphingomyelinase in major depression Rapid Communication. 1583–1590.

Kornhuber J., Muehlbacher M., Trapp S., Pechmann S., Friedl A., Reichel M., Mühle C., et al. (2011) Identification of novel functional inhibitors of acid sphingomyelinase. *PLoS One* **6**, e23852.

Kornhuber J., Müller C. P., Becker K. A., Reichel M., Gulbins E. (2014) The ceramide system as a novel antidepressant target. *Trends Pharmacol. Sci.* **35**, 293–304.

Kornhuber J., Reichel M., Tripal P., Groemer T. W., Henkel A. W., Mühle C., Gulbins E. (2009) The role of ceramide in major depressive disorder. *Eur. Arch. Psychiatry Clin. Neurosci.* **259**, 199–204.

Kornhuber J., Rhein C., Müller C. P., Mühle C. (2015) Secretory sphingomyelinase in health and disease. *Biol. Chem.* **396**, 707–736.

Lamour N. F., Wijesinghe D. S., Mietla J. A., Ward K. E., Stahelin R. V., Chalfant C. E. (2011) Ceramide Kinase Regulates the Production of Tumor Necrosis Factor α (TNFα) via Inhibition of TNFα-converting Enzyme. *J. Biol. Chem.* **286**, 42808–42817.

Lang P. A., Schenck M., Nicolay J. P., Becker J. U., Kempe D. S., Lupescu A., Schmid K. W., et al. (2007) Liver cell death and anemia in Wilson disease involve acid sphingomyelinase and ceramide. **13**.

Lareu R. R., Zeugolis D. I., Abu-Rub M., Pandit A., Raghunath M. (2010) Essential modification of the Sircol Collagen Assay for the accurate quantification of collagen content in complex protein solutions. *Acta Biomater.* **6**, 3146–3151.

Lasarte S., Samaniego R., Salinas-Muñoz L., Guia-Gonzalez M. A., Weiss L. A., Mercader E., Ceballos-García E., et al. (2016) Sex Hormones Coordinate Neutrophil Immunity in the Vagina by Controlling Chemokine Gradients. *J. Infect. Dis.* **213**, 476–84.

Lavieu G., Scarlatti F., Sala G., Carpentier S., Levade T., Ghidoni R., Botti J., Codogno P. (2006) Regulation of autophagy by sphingosine kinase 1 and its role in cell survival during nutrient starvation. *J. Biol. Chem.* **281**, 8518–27.

Laws K. R., Irvine K., Gale T. M. (2018) Sex differences in Alzheimer's disease. *Curr. Opin. Psychiatry* **31**, 133–139.

Lee J. K., Jin H. K., Park M. H., Kim B., Lee P. H., Nakauchi H., Carter J. E., He X., Schuchman E. H., Bae J. (2014) Acid sphingomyelinase modulates the autophagic process by controlling lysosomal biogenesis in Alzheimer's disease. *J. Exp. Med.* **211**, 1551–70.

Lepple-Wienhues A., Belka C., Laun T., Jekle A., Walter B., Wieland U., Welz M., et al. (1999) Stimulation of CD95 (Fas) blocks T lymphocyte calcium channels through sphingomyelinase and sphingolipids. *Proc. Natl. Acad. Sci.* **96**, 13795–13800.

Levine B., Kroemer G. (2008) Autophagy in the Pathogenesis of Disease. *Cell* **132**, 27–42.

Levine B., Mizushima N., Virgin H. W. (2011) Autophagy in immunity and inflammation. *Nature* **469**, 323–335.

Levy M., Futerman A. H. (2010) Mammalian ceramide synthases. *IUBMB Life* **62**, NA-NA.

Lin W.-C., Lin C.-F., Chen C.-L., Chen C.-W., Lin Y.-S. (2011) Inhibition of Neutrophil Apoptosis via Sphingolipid Signaling in Acute Lung Injury. *J. Pharmacol. Exp. Ther.* **339**, 45–53.

Lin X., Li S., Zhao Y., Ma X., Zhang K., He X., Wang Z. (2013) Interaction Domains of p62: A Bridge Between p62 and Selective Autophagy. *DNA Cell Biol.* **32**, 220–227.

Lingwood D., Simons K. (2010) Lipid rafts as a membrane-organizing principle. *Science* **327**, 46–50.

Linke T., Wilkening G., Lansmann S., Moczall H., Bartelsen O., Weisgerber J., Sandhoff K. (2001) Stimulation of acid sphingomyelinase activity by lysosomal lipids and sphingolipid activator proteins. *Biol. Chem.* **382**, 283–90.

Malik F. A., Meissner A., Semenkov I., Molinski S., Pasyk S., Ahmadi S., Bui H. H., Bear C. E., Lidington D., Bolz S.-S. (2015) Sphingosine-1-Phosphate Is a Novel Regulator of Cystic Fibrosis Transmembrane Conductance Regulator (CFTR) Activity. *PLoS One* **10**, e0130313.

Marathe S., Schissel S. L., Yellin M. J., Beatini N., Mintzer R., Williams K. J., Tabas I. (1998) Human Vascular Endothelial Cells Are a Rich and Regulatable Source of Secretory Sphingomyelinase. *J. Biol. Chem.* **273**, 4081–4088.

Matthews W. J., Williams M., Oliphint B., Geha R., Colten H. R. (1980) Hypogammaglobulinemia in Patients with Cystic Fibrosis. *N. Engl. J. Med.* **302**, 245–249.

Michaud J., Kohno M., Proia R. L., Hla T. (2006) Normal acute and chronic inflammatory responses in sphingosine kinase 1 knockout mice. *FEBS Lett.* **580**, 4607–12.

Mikati M. A., Zeinieh M., Abi R., El J., Rahmeh A., El M., Usta J., Dbaibo G. (2008) and caspase-3 during and after experimental status epilepticus.

Miyagi M., Aoyama H., Morishita M., Iwamoto Y. (1992) Effects of sex hormones on chemotaxis of human peripheral polymorphonuclear leukocytes and monocytes. *J. Periodontol.* **63**, 28–32.

Mizumura K., Justice M. J., Schweitzer K. S., Krishnan S., Bronova I., Berdyshev E. V., Hubbard W. C., et al. (2018) Sphingolipid regulation of lung epithelial cell mitophagy and necroptosis during cigarette smoke exposure. *FASEB J.* **32**, 1880–1890.

Molloy E. J., O'Neill A. J., Grantham J. J., Sheridan-Pereira M., Fitzpatrick J. M., Webb D. W., Watson R. W. G. (2003) Sex-specific alterations in neutrophil apoptosis: the role of estradiol and progesterone. *Blood* **102**, 2653–9.

Morell P., Quarles R. H. (1999) The Myelin Sheath.

Mühle C., Huttner H. B., Walter S., Reichel M., Canneva F., Lewczuk P., Gulbins E., Kornhuber J. (2013) Characterization of Acid Sphingomyelinase Activity in Human Cerebrospinal Fluid. *PLoS One* **8**.

Mühle C., Kornhuber J. (2017) Assay to measure sphingomyelinase and ceramidase activities efficiently and safely. *J. Chromatogr. A* **1481**, 137–144.

Mullen T. D., Hannun Y. A., Obeid L. M. (2012) Ceramide synthases at the centre of sphingolipid metabolism and biology. *Biochem. J.* **441**, 789–802.

Müller C. P., Kalinichenko L. S., Tiesel J., Witt M., Stöckl T., Sprenger E., Fuchser J., et al. (2017) Paradoxical antidepressant effects of alcohol are related to acid sphingomyelinase and its control of sphingolipid homeostasis. *Acta Neuropathol.* **133**, 463–483.

Müller G., Ayoub M., Storz P., Rennecke J., Fabbro D., Pfizenmaier K. (1995) PKC zeta is a molecular switch in signal transduction of TNF-alpha, bifunctionally regulated by ceramide and arachidonic acid. *EMBO J.* **14**, 1961–9.

Nährlich, L.; Burkhart, M.; Wosniok J. (2017) *Deutsches Mukoviszidose-Register, Berichtsband 2017*.

Nakatogawa H., Suzuki K., Kamada Y., Ohsumi Y. (2009) Dynamics and diversity in autophagy mechanisms: lessons from yeast. *Nat. Rev. Mol. Cell Biol.* **10**, 458–467.

Nakayama H., Ogawa H., Takamori K., Iwabuchi K. (2013) GSL-enriched membrane microdomains in innate immune responses. *Arch. Immunol. Ther. Exp. (Warsz).* **61**, 217–28.

Netea-Maier R. T., Plantinga T. S., Veerdonk F. L. van de, Smit J. W., Netea M. G. (2016) Modulation of inflammation by autophagy: Consequences for human disease. *Autophagy* **12**, 245–260.

Newton A. C., Bootman M. D., Scott J. D. (2016) Second Messengers. *Cold Spring Harb. Perspect. Biol.* **8**.

Newton J., Lima S., Maceyka M., Spiegel S. (2015) Revisiting the sphingolipid rheostat: Evolving concepts in cancer therapy. *Exp. Cell Res.* **333**, 195–200.

Nixon G. F. (2009) Sphingolipids in inflammation: pathological implications and potential therapeutic targets. *Br. J. Pharmacol.* **158**, 982–93.

Oaks J., Ogretmen B. (2014) Regulation of PP2A by Sphingolipid Metabolism and Signaling. *Front. Oncol.* **4**, 388.

Ohta H., Yatomi Y., Sweeney E. A., Hakomori S., Igarashi Y. (1994) A possible role of sphingosine in induction of apoptosis by tumor necrosis factor-alpha in human neutrophils. *FEBS Lett.* **355**, 267–70.

Okino N., He X., Gatt S., Sandhoff K., Ito M., Schuchman E. H. (2003) The reverse activity of human acid ceramidase. *J. Biol. Chem.* **278**, 29948–53.

Palikaras K., Lionaki E., Tavernarakis N. (2018) Mechanisms of mitophagy in cellular homeostasis, physiology and pathology. *Nat. Cell Biol.* **20**, 1013–1022.

Pan W., Yu J., Shi R., Yan L., Yang T., Li Y., Zhang Z., et al. (2014) Elevation of ceramide and activation of secretory acid sphingomyelinase in patients with acute coronary syndromes. *Coron. Artery Dis.* **25**, 1.

Petrache I., Kamocki K., Poirier C., Pewzner-Jung Y., Laviad E. L., Schweitzer K. S., Demark M. Van, Justice M. J., Hubbard W. C., Futerman A. H. (2013) Ceramide Synthases Expression and Role of Ceramide Synthase-2 in the Lung: Insight from Human Lung Cells and Mouse Models. *PLoS One* **8**, e62968.

Pettus B. J., Bielawska A., Subramanian P., Wijesinghe D. S., Maceyka M., Leslie C. C., Evans J. H., et al. (2004) Ceramide 1-phosphate is a direct activator of cytosolic phospholipase A2. *J. Biol. Chem.* **279**, 11320–6.

Pewzner-Jung Y., Tavakoli Tabazavareh S., Grassme H., Becker K. A., Japtok L., Steinmann J., Joseph T., et al. (2014) Sphingoid long chain bases prevent lung infection by Pseudomonas aeruginosa. *EMBO Mol. Med.* **6**, 1205–1214.

Qiu H., Edmunds T., Baker-Malcolm J., Karey K. P., Estes S., Schwarz C., Hughes H., Patten S. M. Van (2003) Activation of human acid sphingomyelinase through modification or deletion of C-terminal cysteine. *J. Biol. Chem.* **278**, 32744–32752.

Quillin R. C., Wilson G. C., Nojima H., Freeman C. M., Wang J., Schuster R. M., Blanchard J. A., et al. (2015) Inhibition of acidic sphingomyelinase reduces established hepatic fibrosis in mice. *Hepatol. Res.* **45**, 305–14.

Quinn P. J., Wolf C. (2009) The liquid-ordered phase in membranes. *Biochim. Biophys. Acta - Biomembr.* **1788**, 33–46.

Rainville J. R., Tsyglakova M., Hodes G. E. (2018) Deciphering sex differences in the immune system and depression. *Front. Neuroendocrinol.* **50**, 67–90.

Razzaq T. M., Ozegbe P., Jury E. C., Sembi P., Blackwell N. M., Kabouridis P. S. (2004) Regulation of T-cell receptor signalling by membrane microdomains. *Immunology* **113**, 413–426.

Reichel M., Greiner E., Richter-schmidinger T., Tripal P., Jacobi A., Bleich S., Gulbins E., Kornhuber J. (2010) Increased Acid Sphingomyelinase Activity in Peripheral Blood Cells of Acutely Intoxicated Patients. **34**, 46–50.

Rosales C. (2018) Neutrophil: A Cell with Many Roles in Inflammation or Several Cell Types? *Front. Physiol.* **9**, 113.

Rotolo J. A., Zhang J., Donepudi M., Lee H., Fuks Z., Kolesnick R., Biol E. J. (2005) Caspase-dependent and -independent Activation of Acid Sphingomyelinase Signaling *. **280**, 26425–26434.

Sacket S. J., Chung H.-Y., Okajima F., Im D.-S. (2009) Increase in sphingolipid catabolic enzyme activity during aging. *Acta Pharmacol. Sin.* **30**, 1454–61.

Samapati R., Yang Y., Yin J., Stoerger C., Arenz C., Dietrich A., Gudermann T., et al. Lung Endothelial Ca 2 1 and Permeability Response to Platelet-Activating Factor Is Mediated by Acid Sphingomyelinase and Transient Receptor Potential Classical 6. 5.

Sathe M., Houwen R. (2017) Meconium ileus in Cystic Fibrosis. *J. Cyst. Fibros.* **16 Suppl 2**, S32–S39.

Scarpa M. C., Baraldo S., Marian E., Turato G., Calabrese F., Saetta M., Maestrelli P. (2013) Ceramide expression and cell homeostasis in chronic obstructive pulmonary disease. *Respiration* **85**, 342–349.

Scheiblich H., Schlütter A., Golenbock D. T., Latz E., Martinez-Martinez P., Heneka M. T. (2017) Activation of the NLRP3 inflammasome in microglia: the role of ceramide. *J. Neurochem.* **143**, 534–550.

Schissel S. L., Jiang X., Tweedie-Hardman J., Jeong T., Camejo E. H., Najib J., Rapp J. H., Williams K. J., Tabas I. (1998a) Secretory sphingomyelinase, a product of the acid sphingomyelinase gene, can hydrolyze atherogenic lipoproteins at neutral pH. Implications for atherosclerotic lesion development. *J. Biol. Chem.* **273**, 2738–46.

Schissel S. L., Keesler G. A., Schuchman E. H., Williams K. J., Tabas I. (1998b) The cellular trafficking and zinc dependence of secretory and lysosomal sphingomyelinase, two products of the acid sphingomyelinase gene. *J. Biol. Chem.* **273**, 18250–9.

Schissel S. L., Schuchman E. H., Williams K. J., Tabas I. (1996) Zn2+-stimulated sphingomyelinase is secreted by many cell types and is a product of the acid sphingomyelinase gene. *J. Biol. Chem.* **271**, 18431–6.

Schramm M., Herz J., Haas A., Krönke M., Utermöhlen O. (2008) Acid sphingomyelinase is required for efficient phago-lysosomal fusion. *Cell. Microbiol.* **10**, 1839–1853.

Seitz A. P., Grassmé H., Edwards M. J., Pewzner-Jung Y., Gulbins E. (2015) Ceramide and sphingosine in pulmonary infections. *Biol. Chem.* **396**, 611–20.

Settembre C., Ballabio A. (2011) TFEB regulates autophagy: an integrated coordination of cellular degradation and recycling processes. *Autophagy* **7**, 1379–81.

Settembre C., Fraldi A., Medina D. L., Ballabio A. (2013) Signals from the lysosome: a control centre for cellular clearance and energy metabolism. *Nat. Rev. Mol. Cell Biol.* **14**, 283–96.

Sezgin E., Levental I., Mayor S., Eggeling C. (2017) The mystery of membrane organization: composition, regulation and roles of lipid rafts. *Nat. Rev. Mol. Cell Biol.* **18**, 361–374.

Sic H., Kraus H., Madl J., Flittner K. A., Münchow A. L. Von, Pieper K., Rizzi M., et al. (2014) Sphingosine-1-phosphate receptors control B-cell migration through signaling components associated with primary immunodeficiencies, chronic lymphocytic leukemia, and multiple sclerosis. *J. Allergy Clin. Immunol.* **134**.

Simons K., Ikonen E. (1997) 1997Functional rafts in cell membranes..pdf. 569–572.

Simpson M. A., Cross H., Proukakis C., Priestman D. A., Neville D. C. A., Reinkensmeier G., Wang H., et al. (2004) Infantile-onset symptomatic epilepsy syndrome caused by a homozygous loss-of-function mutation of GM3 synthase. *Nat. Genet.* **36**, 1225–1229.

Singer S. J., Nicolson G. L. (1972) The fluid mosaic model of the structure of cell membranes. *Science* **175**, 720–31.

Singh V. K., Schwarzenberg S. J. (2017) Pancreatic insufficiency in Cystic Fibrosis. *J. Cyst. Fibros.* **16**, S70–S78.

Siskind L. J., Colombini M. (2000) The Lipids C_2 - and C_{16} -Ceramide Form Large Stable Channels. *J. Biol. Chem.* **275**, 38640–38644.

Snider A. J., Kawamori T., Bradshaw S. G., Orr K. A., Gilkeson G. S., Hannun Y. A., Obeid L. M. (2009) A role for sphingosine kinase 1 in dextran sulfate sodium-induced colitis. *FASEB J.* **23**, 143–52.

Spiegel S., Milstien S. (2011) The outs and the ins of sphingosine-1-phosphate in immunity. *Nat. Rev. Immunol.* **11**, 403–415.

Stancevic B., Kolesnick R. (2010) Ceramide-rich platforms in transmembrane signaling. *FEBS Lett.* **584**, 1728–1740.

Stein B., Yang M. X. (1995) Repression of the interleukin-6 promoter by estrogen receptor is mediated by NF-kappa B and C/EBP beta. *Mol. Cell. Biol.* **15**, 4971–9.

Straczkowski M., Kowalska I., Baranowski M. (2007) Increased skeletal muscle ceramide level in men at risk of developing type 2 diabetes S1P. 2366–2373.

Sutherland E. W. (1970) On the biological role of cyclic AMP. *JAMA* **214**, 1281–8.

Taniguchi M., Kitatani K., Kondo T., Hashimoto-Nishimura M., Asano S., Hayashi A., Mitsutake S., et al. (2012) Regulation of Autophagy and Its Associated Cell Death by "Sphingolipid Rheostat." *J. Biol. Chem.* **287**, 39898–39910.

Tayama M., Soeda S., Kishimoto Y., Martin B. M., Callahan J. W., Hiraiwa M., O'Brien J. S. (1993) Effect of saposins on acid sphingomyelinase. *Biochem. J.* **290 (Pt 2**, 401–4.

Teichgräber V., Ulrich M., Endlich N., Riethmüller J., Wilker B., Oliveira–Munding C. C. De, Heeckeren A. M. van, et al. (2008) Ceramide accumulation mediates inflammation, cell death and infection susceptibility in cystic fibrosis. *Nat. Med.* **14**, 382–391.

Testi R. (1996) Sphingomyelin breakdown and cell fate. *Trends Biochem. Sci.* **21**, 468–471.

Thudichum J. W. A. (1884) Treatise on the Chemical Constitution of Brain. *Bailliere, Tindall Cox, London* 149.

Varshney P., Yadav V., Saini N. (2016) Lipid rafts in immune signalling: current progress and future perspective. *Immunology* **149**, 13–24.

Veltman M., Stolarczyk M., Radzioch D., Wojewodka G., Sanctis J. B. De, Dik W. A., Dzyubachyk O., Oravecz T., Kleer I. de, Scholte B. J. (2016) Correction of lung inflammation in a F508del CFTR murine cystic fibrosis model by the sphingosine-1-phosphate lyase inhibitor LX2931. *Am. J. Physiol. Lung Cell. Mol. Physiol.* **311**, L1000–L1014.

Voskuhl R. (2011) Sex differences in autoimmune diseases. *Biol. Sex Differ.* **2**, 1.

Wong P.-M., Feng Y., Wang J., Shi R., Jiang X. (2015) Regulation of autophagy by coordinated action of mTORC1 and protein phosphatase 2A. *Nat. Commun.* **6**, 8048.

Xiong Z. J., Huang J., Poda G., Pomès R., Privé G. G. (2016) Structure of Human Acid Sphingomyelinase Reveals the Role of the Saposin Domain in Activating Substrate Hydrolysis. *J. Mol. Biol.* **428**, 3026–3042.

Xu Z., Zhou J., McCoy D. M., Mallampalli R. K. (2005) LASS5 is the predominant ceramide synthase isoform involved in de novo sphingolipid synthesis in lung epithelia. *J. Lipid Res.* **46**, 1229–38.

Young M. M., Kester M., Wang H.-G. (2013) Sphingolipids: regulators of crosstalk between apoptosis and autophagy. *J. Lipid Res.* **54**, 5–19.

Zachari M., Ganley I. G. (2017) The mammalian ULK1 complex and autophagy initiation. *Essays Biochem.* **61**, 585–596.

Zeidan Y. H., Hannun Y. A. (2007) Activation of acid sphingomyelinase by protein kinase C??-mediated phosphorylation. *J. Biol. Chem.* **282**, 11549–11561.

Zhang C., Li P.-L. (2010) Membrane raft redox signalosomes in endothelial cells. *Free Radic. Res.* **44**, 831–842.

Zhang Y., Yao B., Delikat S., Bayoumy S., Lin X., Basu S., Mcginley M., Lichenstein H., Kolesnick R. (1997) Kinase Suppressor of Ras Is Ceramide-Activated Protein Kinase. **89**, 63–72.

Zhou Y. F., Metcalf M. C., Garman S. C., Edmunds T., Qiu H., Wei R. R. (2016) Human acid sphingomyelinase structures provide insight to molecular basis of Niemann-Pick disease. *Nat. Commun.* **7**, 1–10.

Zhou Y., Zhang T., Zhang Q.-K., Jiang Y., Xu D.-G., Zhang M., Shen W., Pan Q.-J. (2014) Unstable expression of transgene is associated with the methylation of CAG promoter in the offspring from the same litter of homozygous transgenic mice. *Mol. Biol. Rep.* **41**, 5177–5186.

Ziobro R., Henry B., Edwards M. J., Lentsch A. B., Gulbins E. (2013) Ceramide mediates lung fibrosis in cystic fibrosis. *Biochem. Biophys. Res. Commun.* **434**, 705–709.

Acknowledgements

First and foremost I want to thank Prof. Dr. Katrin Becker-Flegler for the opportunity to work on this project. I want to thank her equally for her unwavering support, encouraging discussions, and seemingly endless patience throughout my research time as well as during the writing of my thesis. I am more than thankful for having met someone who combines with such ease being joyful and spirited as well as disciplined and compassionate.

I also want to thank Prof. Dr. Erich Gulbins as director of the institute of molecular biology, but even more so as speaker of the GRK 2098, “Biomedicine of the acid sphingomyelinase/acid ceramidase system”, which supported me and many other PhD students. I owe much to the scientific exchange which this research training group provided.

I am very grateful to Prof. Richard Kolesnick and Dr. Adriana Haimovitz-Friedman for their mentoring and support in the time I spent at the Memorial Sloan-Kettering Cancer Center in New York.

Thanks is due to Dr. Fabian Schumacher of the University of Potsdam for conducting all mass spectrometric measurements for this project.

To my fellow (PhD) students I can only say thank you for being by my side, every one of you has brought enrichment and encouragement to my life in your own special way: Nadine Beckmann, Salina Begum, Ulrike Glaser, Karen Hung, Barbara Kovačić, Cao Li, Jie Ma, Valentine Marais, Eyad Naser, Yuqing Wu.

A major thank you is in order to every member of the institute of molecular biology: Dr. Alexander Carpinteiro, Hannelore Disselhoff, Dr. Heike Grassmé, Gabriele Hessler, Dr. Stephanie Kadow, Simone Keitsch, Melanie Kramer, Claudine Kühn, Siegfried Moyrer, Helga Pätsch, Bettina Peter, Bärbel Pollmeier, Andrea Riehle, Ashraf Swaidan, and Barbara Wilker. I would like to thank Carolin Sehl and Matthias Soddemann in particular. I enjoyed a wonderful work environment that included (a lot of) practical and technical help as well as scientific discussions but also lots of laughter and emotional support.

Last but not least, I thank my friends and family. Their unconditional support over the years and the last few months in particular has enabled me to do everything. I’m particularly grateful to Elke Blanck, Imke Goertz und Britta Merz.

Most importantly, I want to acknowledge my parents and grandparents who’ve lifted me up throughout my life.

Truly, I am standing on the shoulders of giants.

Curriculum Vitae

Der Lebenslauf ist in der Online-Version aus Gründen des Datenschutzes nicht enthalten

Declarations

Erklärung:

Hiermit erkläre ich, gem. § 7 Abs. (2) d) + f) der Promotionsordnung der Fakultät für Biologie zur Erlangung des Dr. rer. nat., dass ich die vorliegende Dissertation selbständig verfasst und mich keiner anderen als der angegebenen Hilfsmittel bedient, bei der Abfassung der Dissertation nur die angegeben Hilfsmittel benutzt und alle wörtlich oder inhaltlich übernommenen Stellen als solche gekennzeichnet habe.

Essen, den _____ _____

Unterschrift der Doktorandin

Erklärung:

Hiermit erkläre ich, gem. § 7 Abs. (2) e) + g) der Promotionsordnung der Fakultät für Biologie zur Erlangung des Dr. rer. nat., dass ich keine anderen Promotionen bzw. Promotionsversuche in der Vergangenheit durchgeführt habe und dass diese Arbeit von keiner anderen Fakultät/Fachbereich abgelehnt worden ist.

Essen, den _____ _____

Unterschrift der Doktorandin

Erklärung:

Hiermit erkläre ich, gem. § 6 Abs. (2) g) der Promotionsordnung der Fakultät für Biologie zur Erlangung der Dr. rer. nat., dass ich das Arbeitsgebiet, dem das Thema „Titel der Dissertation“ zuzuordnen ist, in Forschung und Lehre vertrete und den Antrag von (Name des Doktoranden) befürworte und die Betreuung auch im Falle eines Weggangs, wenn nicht wichtige Gründe dem entgegenstehen, weiterführen werde.

Essen, den _____ _____

Prof. Dr. Katrin Becker-Flegler
Unterschrift eines Mitglieds der Universität Duisburg-Essen